Cape Peninsula
University of Technology

THE CONTROL OF A THREE-PHASE PWM REGENERATIVE RECTIFIER

By

FELICIDADE PEMBA KINZO GARCIA

Dissertation submitted in partial fulfilment of the requirements for the

degreeMaster of Engineering: Electrical Engineering

in the Faculty of Engineering

at the Cape Peninsula University of Technology

Supervisor: Dr AK Raji

Bellville
October 2020

DECLARATION

I, Felicidade Pemba Kinzo Garcia, declare that this dissertation/thesis's contents represent my unaided work. The dissertation/thesis has not previously been submitted for academic examination towards any qualification. Furthermore, it expresses my own opinions and not necessarily those of the Cape Peninsula University of Technology.

Signed **Date**

ABSTRACT

The use of renewable generators has increased intensively as a response to global warming. The target is to develop these technologies to diminish the environmental impacts and ensure reliable and cost-effective energy. Wind power is one of the fastest-growing clean energy technologies to replace fossil fuel-based power generation units and support energy security. When using these types of generators, the major challenge is their dependency on weather conditions, causing their power output to be unreliable. In such a case, power electronics converters are used as interfaces between the wind generators and the loads. Depending on the type of loads, power electronics for wind power applications can be either AC to DC (rectifiers) or DC to AC converters (inverters) or a combination of both types (back to back converters). However, this research focuses on AC to DC converters. Two main topologies of AC to DC converters can be found; the line commutated rectifiers and power factor correction rectifiers. The power factor correction rectifiers consist of PWM regenerative and PWM non-regenerative rectifiers. In PWM regenerative rectifiers, a proper control scheme must operate the rectifier efficiently and maintain the output voltage to a stable value.

This study aims to develop a control scheme for a three-phase PWM regenerative rectifier receiving AC power from a 1.53 MW permanent magnet synchronous wind generator at a line voltage of 953 V. The rectifier delivers 1.26 MW at a DC voltage of 1150 V to a DC load connected to its output terminals. The control system scheme adopted in this study is based on a voltage-oriented control strategy. The modelling and simulation are performed using the Matlab/Simulink environment. Three types of loads, namely R, RL, and RC loads, are considered to evaluate the designed controller's performance. The results show a good performance of the designed controller as the output voltage could be maintained close to the set reference value. At the same time, the rectifier delivered 1.26 MW to the load.

ACKNOWLEDGEMENTS

I wish to thank:

- Dr Doud Nanintamo Luta, my advisor for the precious guidance, dedication, support, commitment, and motivation throughout this research,
- My supervisor, Dr Atanda Raji, for his support and guidance,
- Lukenia Gomes, for her support and motivation,
- My pastor Marcio David, for all the spiritual support and motivation throughout this research,
- I also express my gratitude to Suilety Berta, Zenaide Luis, Elizandra Alfredo, Rosimer Arcanjo, Ana Chissano, Domingos Antonio, and all church members.

DEDICATION

I dedicate this work to my parents, Garcia Joao Miguel Dago and Maria Kinzo Isaias Dago, and my siblings (Isabel Sita Dago, Helena Kinzo Garcia, Antonio Saldanha, Sita Saldanha, Eva Saldanha, Marta Saldanha, Miqueias Saldanha).

LIST OF FIGURES

LIST OF TABLES

TABLE OF CONTENTS

GLOSSARY

AC	Alternating Current
CSR	Current Source Rectifier
CSP	Concentrating Solar Power
DC	Direct Current
DPC	Direct Power Control
RE	Renewable Energy
PV	Photovoltaic
R&D	Research and Development
m/s	Meter Per Second
IEC	International Electromechanical Commission
IGCT	Integrated gate-commutated thyristor
kW	Kilowatt
MW	Megawatt
GW	Gigawatt
HAWT	Horizontal Axis Wind Turbines
PMSG	Permanent Magnet Synchronous Generator
PWM	Pulse Width Modulation
SVPWM	Space Vector Pulse Width Modulation
VAWT	Vertical Axis Wind Turbine
VFOC	Virtual-flux Oriented Control
VF-DPC	Virtual-flux Direct Power Control
VOC	Voltage Oriented Control
VSR	Voltage Source Rectifier
PLL	Pulse phase Locked Loop
TWh	Terawatt hour
WT	Wind Turbine
WEC	Wind Energy Conversion
IGBT	Insulated Gate Bipolar Transistor
SHE	Selective Harmonics Elimination
HB-PWM	Hysteresis Band Pulse Width Modulation
SPWM	Sinusoidal Pulse Width Modulation
SVPWM	Space Vector Pulse Width Modulation
IEC	International electromechanical Commission
PI	Proportional and Integral Controller
ω_n	Natural Frequency
V_{OC}	Open Circuit Voltage

I_{SC}	Short Circuit Current
MPP	Maximum Power Point
FF	Fill Factor
V_{mp}	Voltage Corresponding to MPP
I_{mp}	Current Corresponding to MPP
P_{max}	Maximum Output Power
P_{in}	Input Power of the Module
P_t	Wind Kinetic Power
A	Swept area
ρ	Air Density
R	Radius of the Rotor
λ	Tip Ratio
β	Pitch Angle
C_p	Wind Coefficient
P, P_M	Power of Wind turbine
P_v	Power of the Wind
ω	Rotational Frequency
T_t	Torque
ω_r	The Rotor Speed
V_{cut}	The Cut in Wind Speed
V_{rated}	Rated Wind Speed
P_r	Rated Power
Φ_{nom}	Nominal Magnetic Flux
V_{nom}	Nominal Voltage
ω_{nom}	Generator Angular Velocity
Φ	Magnetic Flux
ϕ_{pu}	Magnetic Flux Per Unit Value
P_{nom}	Nominal Power of the Round Rotor
I_{nom}	Nominal Current
V_{nom}	Nominal Voltage
Z_{nom}	Nominal Impedance
R_S	Stator Resistance
R_{spu}	Resistance Per Unit Value
L_{nom}	Nominal Inductance of the Round Rotor
L_{dq}	Inductance of a Round Rotor in the dq0 Frame
L_{dq_pu}	Inductance Per Unit Value
J	Moment of inertia

N_p	Number of Pole Pairs
H	Inertia Constant
Ω_R	Optimal Rotational Speed
$\lambda_{optimal}$	Optimal Speed Ratio
V_{wind}	Wind Turbine Speed
L_s	Line to Line Inductance
I_{ra}, I_{rb}, I_{rc}	Rectifier Input Current
V_a,V_b,V_c	Three-Phase Voltage Source
$V_{ra}, V_{rb,}V_{rc}$	Rectifier Input Voltages
S_a, S_b, S_c	Switching Functions
V_α, V_β	Voltage in the $\alpha - \beta$ Frame
V_d,V_q	Voltage in the d-q Frame
i_d, i_q	Current in the d-q Frame
V_{DC-min}	Minimum DC-link Voltage
E_m	AC generator Peak Voltage
T_s	Sampling Period
ΔI_{max}	Maximum Ripple Current
$V_{LN(rms)}$	Line to Ground Voltage
$V_{LN(rms)}$	Line to Line Voltage
V_{DC}	DC Bus Voltage
C_{DC}	DC-Link Capacitor
f	Generator Frequency
P	Active Power
TF_v	Transfer Function of the Outer Loop Control
k_{pv}	Proportional Gain
T_{iv}	Time Integrator in the Outer Voltage Loop
f_s	Sampling Frequency
TF_i	Transfer Function of the Inner Loop Control
k_{pi}	Proportional Gain
T_{ii}	Integration Time Constant of Inner Loop Control
$m_d{}^*, m_q{}^*$	Modulation Signals in the d-q Frame
V_{gd},V_{gq}	Disturbance from Input Power Transmission
u_d, u_q	Current errors Output Signals
K_1	Proportional Loop Filter
K_2	Proportional Corresponding Integral Gain

CHAPTER ONE

INTRODUCTION

1.1. Background

During the last two decades, the electricity demand has become higher due to industrial progress and population growth worldwide. An investigation conducted on the power consumption and economic development of 274 cities reveals that these cities need to minimize their energy utilization by more than 25%. The study concluded that if no mitigation actions are taken, the energy use will rise by more than three times between 2005 and 2050 (Thorpe, 2015). Furthermore, with suitable urban design and transport rules, the future increase in urban energy would be limited to 150 000 TWh in 2050, thus decreasing the potential of climate change. Moreover, these cities would need to implement more policies to reduce urban greenhouse gas emissions (Thorpe, 2015). The questions come in how these issues will be solved, what kinds of energy sources and technologies will be used to meet such amount (Stephen, 2017).

Today's electricity market still relies on fossil fuel, which includes coal, gas, and oil, to meet the load demand. However, these energy sources are disadvantageous, as they can release an important quantity of carbon dioxide into the atmosphere, and potentially increasing the risks of global warming. Moreover, it is notable that those sources are running out and will probably cause energy shortage in the next three decades (Ellabban et al., 2014; Stephen, 2017). Other energy technologies such as wind, solar, hydro, biomass, etc., have been developed to address the presented issues. The target is to develop these renewable technologies until energy sources based on fossil fuels are replaced (Stephen, 2017).

The most challenging problem so far when dealing with these renewable technologies is their dependency on weather conditions, questioning their reliability. For instance, in the case of photovoltaic systems, the concerns are related to energy supply's power quality and security. For years, R&Ds has been ongoing to increase the reliability of these technologies. One of the fields that may influence the successful development and operation of renewable generators is power electronics. Indeed, power converters play a huge role in integrating renewable generators into the existing power systems as they are used as interfaces between renewable generators and utility grids or renewable generators and loads.

In the case of wind generators, power converters are used to improve and maintain the power quality that is delivered to electrical loads. There is a great necessity to control

and enhance each related variable of wind generation systems (active and reactive power, output voltage and frequency). For example, to control these variables, in a variable speed wind turbine, a back-to-back converter, which consists of a rectifier circuit, DC to DC boost or buck converter, the inverter may be employed (Phankong et al., 2014).

In general, a back-to-back converter serves as an interface between the wind power system and the grid. Its operation may involve three stages; in the first stage, the generator's output voltage is rectified, the second stage is the DC-link, which connects the rectifier and the inverter. The DC-link capacitor provides a stable voltage, reduces the ripples, and increases the converter (Scapini et al., 2018). Lastly, the inverter converts back the DC voltage to AC voltage with a regulated voltage and frequency.

For an AC wind power system supplying a DC load, only a rectifier is utilised to convert the generated AC power in DC. These rectifiers can be classified into two categories, namely line commuted and power factor correction rectifiers. Line commuted rectifiers are based on diodes and thyristors, whereas the power factor correction rectifiers can be classified into regenerative and non-regenerative rectifiers. Non-regenerative rectifiers are used in power generation to provide the desired voltage and converts a low-level DC voltage to a high-level DC voltage. They include Vienna and boost topologies.

On the other hand, regenerative rectifiers can provide power regeneration depending on the applications. Power is not only supplied from the AC source to the DC load through the rectifier but can also be supplied from the DC to the AC side. Regenerative rectifiers can be of voltage source or current source types. In voltage source rectifiers, power flow from AC to DC in view that the DC voltage moves out across the capacitor, which reflects as the rectifier input terminals, modulated by the switching purpose (Bhattacharya, 2014). Similarly, as a current source with a continuous current at the input side and use a filter capacitor at the output side to commutate the current.

Regenerative rectifiers use power electronics switches like Insulated Gate Bipolar Transistors (IGBT) and MOSFET to change the input current and any related variable. Hence, there is a necessity to apply a proper control scheme to drive the system. Therefore, this research deal with the control of a regenerative rectifier for wind power applications.

1.2. Statement of Research Problem

Various applications using wind power require a power regeneration so as depending on the conditions, the power could flow from the AC to the DC side. This can only be achieved through proper control of the rectifier; this study's problem is the control of a three-phase PWM regenerative rectifier.

1.3. Objectives of the Research

The research aims to develop a control scheme for a three-phase PWM regenerative rectifier receiving power from a permanent magnet synchronous wind generator and connected to a DC load.

Specific objectives consist of:

- developing the system Simulink model,
- developing the controller Simulink model,
- integrating the designed controller into the system's Simulink model,
- simulating the overall system.

1.4. Methodology

The methodology adopted in this research include the following:

- A review of literature on renewable technologies and more specifically on wind power generation technologies as well as power electronics converters for wind power applications and their control,
- The development of mathematical models of the components involved in the system,
- Using power electronics control theories, design a suitable controller for the regenerative rectifier,
- The development of the system's Simulink model based on component mathematical models,
- The analyses of the results.

1.5. Significance of the Research

Power electronics converters are intensively used in renewable power systems. In the case of wind power generation, these converters may increase the system's reliability. A well-designed and controlled topology would be an advantage for the system's functionality. When a system is operating accordingly, it can guarantee power quality

and energy supply security. This study aims to develop a control scheme for a three-phase PWM regenerative rectifier for a wind power plant application. The system topology consists of a rectifier receiving AC power from a 1.53 MW permanent magnet synchronous wind generator at a line voltage of 953 V. Then, the rectifier feeds 1.26 MW at a DC voltage of 1150 V to a DC load connected to its output terminals. The control system scheme adopted in this study is based on a voltage-oriented control strategy. The modelling and simulation are performed using Matlab/Simulink environment.

1.6. Outline of the Research

This thesis is organized as follows:

Chapter 1 provides the background, the problem statement, the objectives, and the significance of the research.

Chapter 2 is dedicated to the literature review on renewable power technologies and wind power generation. A study on PWM regenerative rectifiers and their controls is also carried out.

Chapter 3 covers the system description, the modelling of components involved in the system, and the adopted modelling control schemes.

Chapter 4 focuses on presenting the results obtained from the simulation.

Chapter 5 is dedicated to the conclusion and recommendation.

1.7. Publications

1.7.1. Conference Proceedings

- Garcia, F.P.K. and Raji, A.K., A 100% Renewable CHP System for a Remote Area Power Supply (November 26, 2019). AIUE Proceedings of the 17th Industrial and Commercial Use of Energy Conference 2019, The Riverclub, Cape Town, ISBN 978-0-6399647-4-4, Available at SSRN: https://ssrn.com/abstract=3638141.
- F. P. K. Garcia and A. K. Raji, "Access to Efficient and Sustainable Energy: Case of Madagascar," *2020 IEEE PES/IAS PowerAfrica*, Nairobi, Kenya, 2020, pp. 1-5, doi: 10.1109/PowerAfrica49420.2020.9219881.

CHAPTER TWO

LITERATURE REVIEW

This chapter deals with the literature review on renewable power technologies and, more specifically on wind power generation. Additionally, a section on PWM regenerative rectifiers and their controls is also considered.

2.1. Renewable Power Technologies

Renewable energy refers to natural energy sources that are clean and continuously replenished. They can be used as primary energy in various applications, including cooling, heating, power generation, etc. (Figure 2.1). The most common renewable sources include hydro energy, ocean energy, geothermal energy, solar and wind energy.

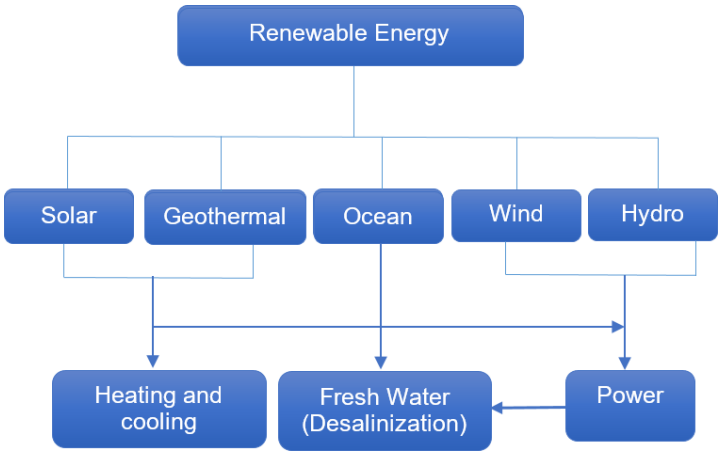

Figure 2.1: Renewable energy sources. (Bilgili et al., 2015)

2.1.1. Hydropower Generation

Hydropower uses moving water from a high elevation to a lower to drive a turbine coupled to a generator, thus generate electricity. The benefits of typical hydropower include pollution-free, the ability to be quickly upgraded, a high capability to store energy for many hours, and a relatively economical and long physical lifetime (Dincer & Acar, 2015). In contrast, their drawbacks include potential displacement of the population from their home due to the construction (Owusu & Asumadu-Sarkodie, 2016) and impacts on local ecosystems (risk of droughts, dry seasons, and changes in local water and land) (Dincer & Acar, 2015).

Hydropower plants come in different sizes, such as large, small, micro, and pico. Their capacity ranges are as follows (Darbellay, 2014):

- Pico hydropower: less than 5 kW,

- Micro hydropower: from 5 kW to 100 kW,
- Small hydropower: from 100 kW to 10 MW,
- Large hydropower: more than 10 MW.

On the other hand, hydropower can also be classified according to the storage capacity, such as impoundments (reservoir type), run-of-river, and pumped storage (Egré & Milewski, 2002). Figure 2.2 shows the schematic of pumped storage, and Table 2.1 presents hydroelectric plant characteristics.

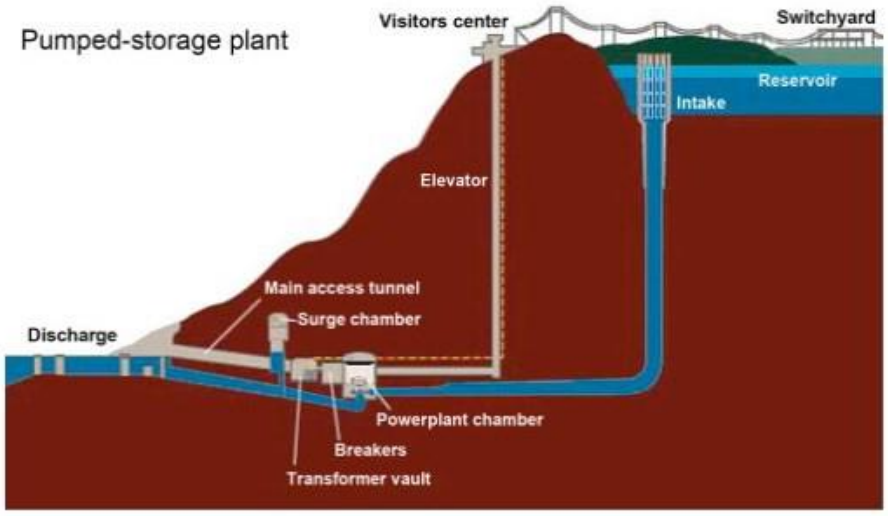

Figure 2.2: Schematic of Pumped hydropower. (Towler, 2014)

Table 2.1: Hydroelectric plant characteristics. (Sarasu et al., 2007; Egré & Milewski, 2002)

Plant types	Service provided	Drawbacks
Impoundments type	• Energy and power	• Changes in habits and social impacts due to the reservoir • Modification of the river flows
Run-of-river	• Based load with reduced flexibility	• Reduced flooding • River flows unchanged
Pumped-storage	• Only power • Net consumer of energy	Effects related to the upper storage pool
Cross-watershed diversion	• Energy only	• Reduction of flow downstream of the diversion • Increase of flow in receiving stream
Upgrading	• Extends project life, sometimes with increased output	• Few additional impacts
Multipurpose	• Hydropower and other water use	• Impacts due to reservoir • Need to evaluate cumulative impacts of other water uses
In-stream diversion	• Energy and power	• Reduction of flow downstream of diversion

2.1.2. Ocean Power Generation

Ocean energy refers to various forms of renewable energy generated from the motion of seawater. This type of technology is still developing; however, it is currently considered an immature technology. In its development, ocean energy doubled the global power capacity in 2011 with approximately 254 MW (Darbellay, 2014). In 2012, this technology was within the ranking of the most used energy source contributing at least 5% to some developed countries' energy matrix. It is expected an increase by 15% over the next 22 years (Darbellay, 2014).

Ocean power technologies can be categorized into wave power, tidal power, and ocean thermal power (Liu, 2015). Wave energy results from the wind as it blows across the surface of the sea. Energy from waves is captured by devices that are stationary or move up and down with the waves' frequency to produce electricity (Darbellay, 2014).

The tidal power is produced by the ebb and flow movement made by the sun and moon's gravitational pull. The generation of electricity is achieved using the mechanical power from seawater's horizontal movement resulting from the density and pressure caused by the unequal division of seawater gradients and salinities. Table 2.2. shows some existing tidal power stations, their locations, and capacities.

Table 2.2: Global tidal power station. (Kuang et al., 2012)

Country	Tidal Power Station	Full Installed Capacity MW
South Korea	Shiwa Lake	254
Russia	Mezen	1.7
South Korea	Undolmok	1.5
Canada	Annapolis Royal	20
France	Rance	240
United Kingdom	Meygen	398
China	Jiangxia	3.2
United Kingdom	Stanford Laugh Seagen	1.2

Lastly, the ocean thermal energy conversion system produces energy by harnessing the temperature gradient between the superficial and deep ocean waters. This temperature gradient is used to drive a turbine, hence produce electricity. A typical ocean thermal energy conversion system's standard layout is depicted in Figure 2.3 (EIA- US Department of Energy, 2019).

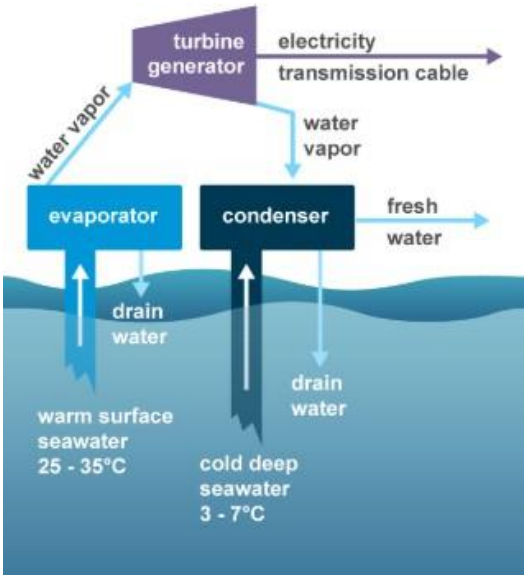

Figure 2.3: Ocean thermal energy system. (EIA- US Department of Energy, 2019)

2.1.3. Geothermal Power Generation

Geothermal energy refers to a potent and efficient way of extracting heat contained into the earth's interior by natural processes. This earth heat can be found anywhere globally on a small scale to provide heat for heating spaces (residential units through heat pumps) or on a large scale (high temperature) for electricity production through a geothermal plant. However, the high temperature needed to drive a power generation station is scarce and can only be found in few places (Ellabban et al., 2014; DiPippo, 2015).

Figure 2.4: Installed capacity of geothermal power in the world. (Richter, 2019)

Figure 2.4 shows the geothermal installed power capacity worldwide in 2019; the USA led the market with 3,639 MW, Indonesia with 1,948 MW, followed by the Philippines 1,868 MW and the rest of the world African, Asian, and North American countries. Geothermal power is expected to reach 150 GW by 2050 (Ellabban et al., 2014).

2.1.4. Solar Power Generation

Solar power generation refers to solar energy use to generate electricity through solar thermal processes and the solar photovoltaic method.

2.1.4.1. Solar thermal power generation

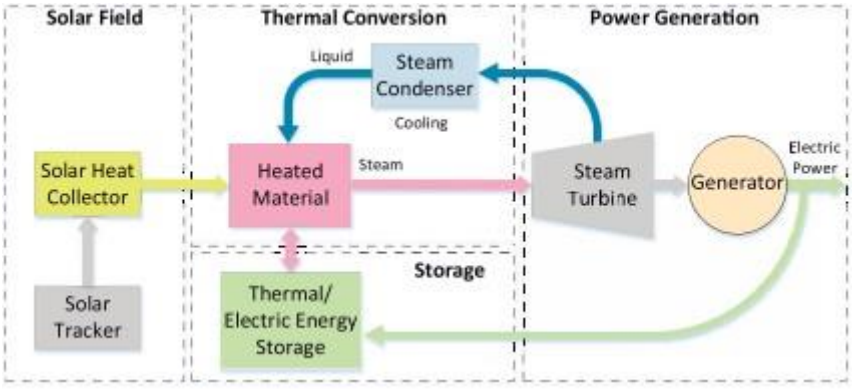

Figure 2.5: Process of generating electricity in solar thermal systems. (Malinowski et al., 2017)

Solar thermal power consists of extracting, concentrating, and using heat from the sun to drive a turbine coupled to an electrical generator. Solar thermal power comprises four types of processes: parabolic through collectors, solar power tower, linear Fresnel reflectors, and parabolic dish systems (Breeze, 2016b). CSP uses oil or steam to transfer solar energy to the power block. The process of generating electricity through solar thermal energy is depicted in Figure 2.5 (Bilgili et al., 2015).

The worldwide capacity installed solar thermal power is still at a lower level since photovoltaic systems reduce the impact of this technology due to their higher installation and running costs and higher sensitivity to dust and humidity (Malinowski et al., 2017).

2.1.4.2. Photovoltaic Power Generation

Photovoltaic refers to the use of solar cells to directly convert sunlight into electricity. These cells are made from various semiconductor materials: silicon, gallium arsenide, cadmium telluride, and copper indium gallium selenide. Three principal photovoltaic cells are widely available: monocrystalline silicon, polycrystalline silicon, and thin film.

A single cell generates about 0.5 to 0.6 V. Hence cells are connected in series, and parallel to increase the voltage and current and form modules with a rated power ranging from 225 to 350 W. Modules are connected in series to form strings. Strings can be connected in parallel to obtain arrays.

Photovoltaic technologies have been desirable worldwide because of their several advantages: noiseless operation, accessible design and installation, long lifetime, less maintenance requirement, and cost-effectiveness (Chakraborty & Kramer, 2013). However, the technology may present some disadvantages such as high initial installation cost, uncertain power output, absence of cost-effective energy storage, etc. (Luque & Hegedus, 2011).

2.1.4.2.1. Photovoltaic Module Characteristics

Characteristics of a photovoltaic module include the short-circuit current, open-circuit voltage, maximum power, fill factor, and efficiency.

a) Open-Circuit Voltage

The open-circuit voltage (V_{OC}) depicted in Figure 2.6 corresponds to the voltage obtained when the current equal to zero. It occurs when the positive and negative terminals are not connected to any load.

b) Short-Circuit Current

The short circuit (I_{SC}) represents the maximum current that occurs when the voltage across the solar cell is equal to zero (Figure 2.6). Its value varies depending on the irradiance.

c) Maximum Power Point

A maximum power point (MPP) is when the solar module supplies its maximum power. It is represented in Figure 2.6 by the curve's knee in which current and voltage result in MPP. The voltage and current corresponding to the MPP are V_{mp} and I_{mp}, respectively.

d) Fill factor

The fill factor FF is the ratio of the maximum output voltage to the product of the short circuit current and the open-circuit voltage as expressed in Equation 2.1.

$$FF = \frac{I_{mp} \times V_{mp}}{I_{SC} \times V_{OC}}$$

Equation 2.1

e) Efficiency

The efficiency is the ratio between the maximum output power to the input power of the module.

$$Efficiency = \frac{P_{max}}{P_{in}}$$

Equation 2.2

where, P_{max} is the maximum output power whereas P_{in} is the input power of the module.

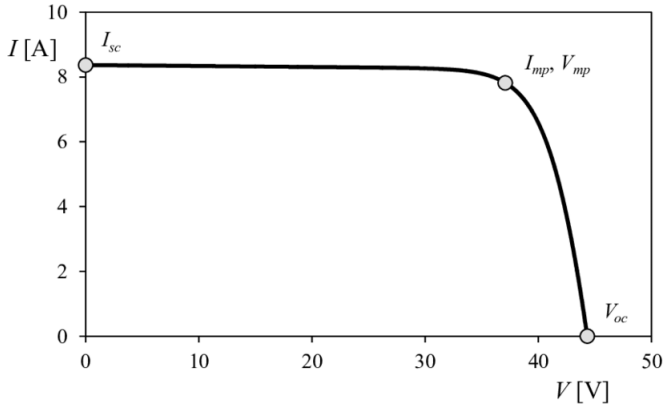

Figure 2.6: I-V curve of photovoltaic modules. (Cubas et al., 2014)

2.1.4.2.2. Photovoltaic System

A PV system can operate in three different configurations, namely grid-connection, off-grid, and hybrid configuration.

a) PV Grid-connected systems

In a grid connection topology, the system is composed of PV arrays connected to the utility grid through a power conditioning unit (PCU). In such a case, the PV system operates in parallel with the utility grid. The PCU includes a DC-to-DC converter driven from a maximum power point (MPPT) algorithm and an inverter including a control system for an efficient system response (see Figure 2.6). Two grid-connected PV configurations can be found; one may include an energy storage device, and the other may not have a backup capability (Vázquez & Vázquez, 2018).

b) Off-Grid PV Systems

Off-grid PV systems are generally installed in remote areas where the electricity from the grid is not accessible. However, such systems can also be implemented in cities to power homes, street lighting, and lanterns (Mohanty et al., 2016). Besides the PV arrays and PCU, this configuration always includes a backup energy storage system to

ensure energy security even when the PV system generates less or is not generating energy.

c) PV Hybrid Systems

In a hybrid configuration, the system consists of PV arrays and other generators such as wind, biomass, or diesel to meet the energy demand. Of the three topologies, the hybrid configuration is more reliable because it depends on multiple energy sources.

2.1.5. Wind Power Generation

Wind power represents a significant and growing source of power from renewable sources after hydroelectricity (Stephen, 2017; Blaabjerg & Ma, 2017). It consists of converting wind energy into electricity through an electric generator. The technology can be installed either onshore or offshore and has the following advantages (Letcher, 2017):

- pollution-free technology,
- can be installed in a minimal land area,
- plants do not cause risks to surrounding facilities,
- allow users not to have power shortage or failure as experienced by utility grid customers,
- fewer maintenance requirements.

On the other hand, their disadvantages are (Bhatia, 2014):

- their intermittency,
- noise pollution and negative impact on the ecosystem,
- bird flying mortality,
- installation cost depends on the site selection, foundation height, and the output power rating.

2.1.5.1. Wind Power Classification

Wind power can be classified according to the following considerations (Tong, 2010; Letcher, 2017):

- power capacity,
- constructional design,
- installation location,
- power supply mode.

2.1.5.2. Power Capacities

The wind power capacities can range from micro, small, medium, large to ultra-large. Micro wind turbines are mainly employed in rural areas with no access to the utility grid. They are used to power water pumping systems, street lighting, and house appliances in such a case. They operate with low cut-in speeds at the start-up and function with rated power in the range of less than kilowatts (Luta, 2014).

On the other hand, small wind turbines have lower than 100 kW capacities as defined by the International Electromechanical Commission (IEC) Standard 61400-2 (Jonkman et al., 2003; Pourrajabian et al., 2015). They are often operated in standalone mode. Additionally, they can be used to power residential houses, farms, and some particular remote applications like water pumping systems and telecom sites (Poulopoulos & Inglezakis, 2016; Letcher, 2017).

Medium wind turbine rated power is in the range from 100 kW to 1 MW. They can be used for village power, distributed power hybrid systems, and power plants in an on-grid or off-grid configuration (Mittal et al., 2010). The rated power of large wind turbines is up to 10 MW, suitable for utility usage, particularly in offshore areas (Goh, 2019). Lastly, ultra-large wind turbines have a power output of more than 10 MW (Bensalah et al., 2018).

2.1.5.3. Constructional Design

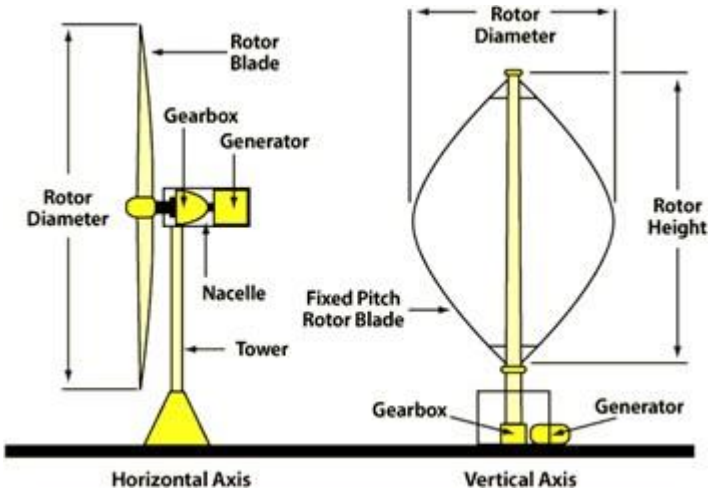

Figure 2.7: Vertical Axis versus Horizontal axis turbine. (Cao et al., 2012; Nayar et al., 2011)

Based on the constructional setup, wind power can be classified as horizontal axis wind turbines (HAWT) and vertical axis wind turbines (VAWT) (Figure 2.7) (Tawfiq et al., 2019).

2.1.5.3.1. Vertical Axis Wind Turbines (VAWT)

In a VAWT, the rotor shaft is set upright and can capture wind from any direction (Shahariar & Hasan, 2014). Moreover, the vertical axis does not need an additional mechanism to face the wind, and heavy generator equipment can be placed on the ground to reduce the tower load (Schubel & Crossley, 2012). The VAWT presents some advantages such as few moving parts simplifying the installation and maintenance, and raising the turbine efficiency; low blade speed, less noise due to the low speed and less visual interference, because of the horizontal movement; no need for additional control compared to the horizontal axis. However, the main disadvantage is the relatively more minor efficiency with slower rotation due to short towers (Tawfiq et al., 2019; Shahariar & Hasan, 2014).

2.1.5.3.2. Horizontal Axis Wind Turbines (HAWT)

The HAWT is the most commercial type of wind turbine, in which the axis of the blade rotation is parallel to the ground and the wind flow. The rotor diameter and the tower's height are very significant in this type of technology as the rotor diameter defines the critical area to obtain the specific power output (Tong, 2010). Two kinds of HAWTs can be found, the upwind turbines and the downwind turbines.

a) Upwind Turbines

Upwind turbines are the most widespread type of horizontal wind turbines in which the rotors face the wind (Pao & Johnson, 2011). Their primary advantage is avoiding the distortion of the flow field while the wind moves through the tower. Their disadvantage is that the rotor must be inflexible and placed far away from the tower. Furthermore, the machine has a yaw mechanism to ensure that the rotor faces the wind.

b) Downwind Turbines

In downwind turbines, the wind flows through the nacelle, tower, and consequently to the rotor blades. In contrast with the upwind topology, the rotors of downwind turbines are more flexible. Their drawback is the output power fluctuation due to the rotor passing through the tower's wind shade. Besides, the downwind machine is somehow built lighter than an upwind engine (Tong, 2010; Karimirad, 2014).

2.1.5.4. Installation Location

Concerning their location, wind power systems can be classified as onshore or offshore systems. Both technologies are similar. However, onshore wind turbines are no longer attractive because of wind availability at the selected locations and population resistance to implementing such technology as it may cause population displacement (Hevia-Koch & Jacobsen, 2019). On the other hand, offshore wind turbines are gaining more interest as these technologies do not require the population's relocation. These plants are constructed in oceans with higher wind speeds availabilities. One of the relevant differences with energy capture is that offshore wind turbine's physical size is bigger than the onshore wind (Breeze, 2016a).

2.1.5.5. Grid-Connected and Off-Grid Wind Turbines

A wind turbine can operate tied or no tied to the grid based on the power supply mode. When it is not connected to the grid, it is referred to as an off-grid turbine; on the contrary, it is grid-connected.

a) Off-Grid Wind Turbine

Like off-grid PV systems, off-grid wind turbines are generally installed in remote areas where the grid's electricity is not accessible. However, such systems can also be implemented in cities to power homes, street lighting, and lanterns (Mohanty et al., 2016). An off-grid wind turbine always includes a backup energy storage system, and, in some cases, they operate in a hybrid configuration.

b) Grid-Connected Wind Turbine

Grid-connected wind power turbines are medium or large-scale wind power generation tied to the grid. They do not require energy storage devices as the grid may supplement any deficit of power to meet the load demand when the system generates a small amount or does not generate power. In case the local load is lesser than generated power, the excess power can be sold to the grid (Tong, 2010).

2.1.5.6. Wind Turbines Component Description

A typical wind power system's components are shown in Figures 2.8, consisting of the generator, rotor blade, Gearbox, nacelle, pitch angle, and tower, including the converter. Those elements are part of wind turbines either in the horizontal axis or vertical axis topology.

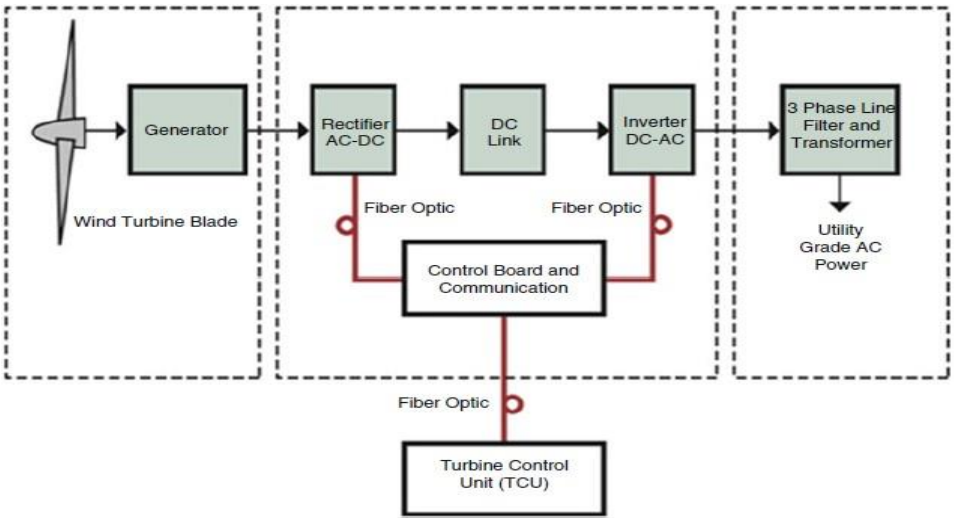

Figure 2.8: Wind turbine component block diagram. (Sumathi et al., 2015)

2.1.5.6.1. Rotor

The rotor consists of a hub and large blades like an airplane wing. It captures wind energy and transfers its power to the rotor hub. The rotor blades are enormous, and usually, turbines consist of three blades; however, two blades are also efficient (Kumar et al., 2016). Three bladed wind turbines are aerodynamically efficient and have low noise, while two blades wind turbines have a higher hub, and the whole structure is more elevated than three-bladed wind turbines. These blades are the rotating component of the system based on the principle of lift and drag. The energy in the wind turns the blades round a rotor. And the rotor is connected to the main shaft, the low-speed shaft, which spins a generator to produce electricity.

The rotor coil is usually made of two or even more wooden fiberglass or steel blades that rotate an axis, either horizontal or vertical, at a rate determined by the wind velocity and the blades' design (Sumathi et al., 2015).

2.1.5.6.2. Gearbox

The gearbox is used in wind turbines to raise rotational speed from a low-speed shaft to a higher rate to make the generator operational. The turbine speed is usually less than 100 RPM, but most generators operate in a range of 1000 to 3600 RPM (Kumar et al., 2016).

2.1.5.6.3. Nacelle

The nacelle is the wind turbine's covered part over the turbine tower's top (Figure 2.9). The nacelle is connected to the rotor, and it supports many components of the wind turbines, such as the rotor shaft, Gearbox, and generators. It is attached to the tower with bearings and can rotate concerning the wind direction to obtain maximum wind

energy (Kumar et al., 2016; Karimirad, 2014). The kinetic energy conversion to electricity occurs on the nacelle rotor. Hence, the rotor nacelle assembly is an essential part of a wind turbine. It protects the wind turbine's components from many weather conditions and reduces noise produced from wind turbines rotation (Karimirad, 2014).

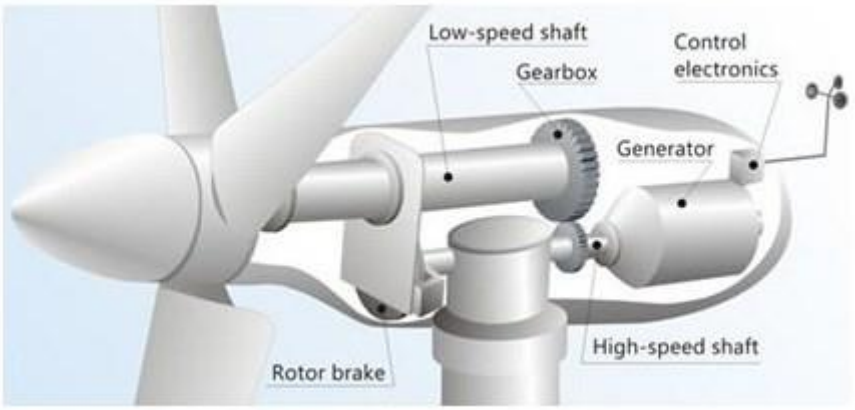

Figure 2.9: Nacelle structure. (Cao et al., 2012)

2.1.5.6.4. Towers

The tower helps to use the wind turbine at sufficient heights above ground. A typical tower supports the wind turbine structures. It also absorbs and securely discharges static and dynamic stress applied on the rotor, the power train, and the nacelle. As wind speed increases with height, taller towers enable turbines to capture more energy and generate more electricity (Sumathi et al., 2015).

2.1.5.7. Wind Turbine Technologies

Based on the generator's design, wind turbines can be grouped as fixed and variable speed wind turbines (Bhowmick & Narvekar, 2018).

2.1.5.7.1. Variable Speed Wind Turbine

Variable-speed operation is obtained by using power electronic converters to decouple the grid and mechanical rotor frequencies. Variable-speed wind turbines are designed to realize maximum aerodynamic efficiency for a variety of wind speeds. It is possible to continuously change the wind turbine's rotational speed to the wind speed (accelerate or decelerate). The turbine may always function at its highest level of aerodynamic efficiency. Three types of variable speed wind turbines can be found: type two, type three and type four.

a) Type Two

A type two wind turbine consists of a wound rotor induction generator connected to a step-up transformer. As shown in Figure 2.10, this type of wind turbine also comprises

a variable resistor in the rotor circuit that controls the rotor current, resulting in constant power output (Sumathi et al., 2015).

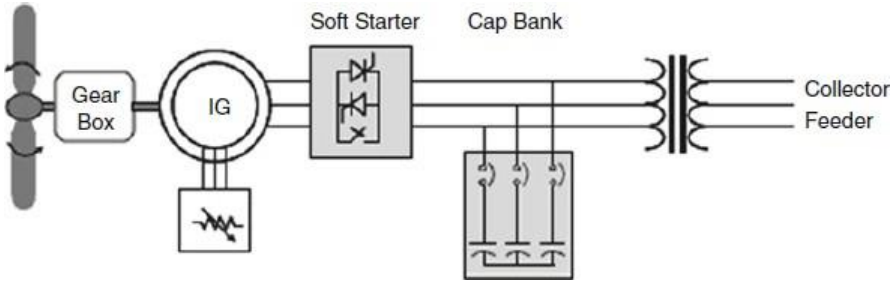

Figure 2.10: Wound rotor induction generator. (Sumathi et al., 2015)

b) Type Three

The Doubly Fed Induction wind turbine (DFIG) is also known as a type three generator. It consists of a stator directly tied to the grid via a transformer. Its rotor is linked to the grid through a power electronic converter (Figure 2.11) with roughly 30% of the generator's power capacity (Sumathi et al., 2015).

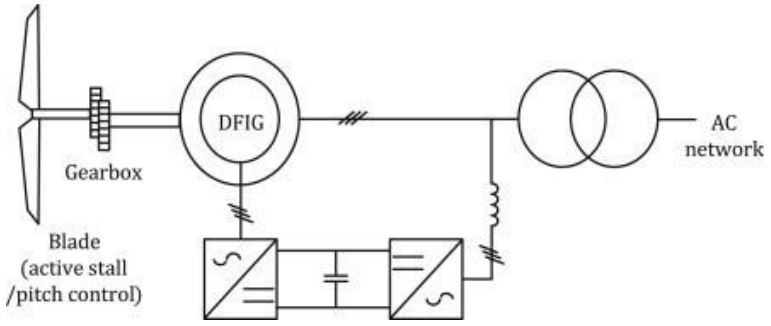

Figure 2.11: Doubly Fed Induction Generator. (Liang & Feng, 2015)

c) Type Four

The type four wind turbine consists of either a wound rotor synchronous machine, or a permanent magnet machine, or an induction machine (Figure 2.12). The generator-side converter rectifies the machine's variable frequency power while the line-side converter inverts the resulting DC power to be injected into the grid (Walling et al., 2012; Hansen & Margaris, 2014). The power converter used is referred to as a full-scale back-to-back frequency converter.

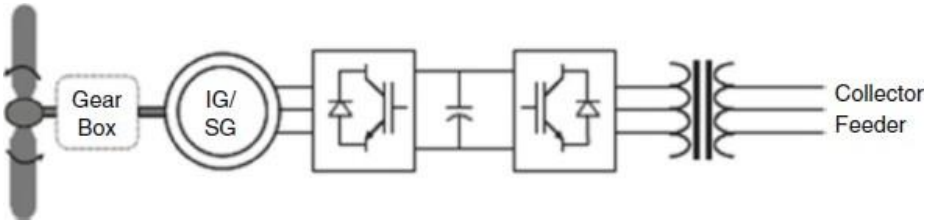

Figure 2.12: Type four wind turbine generator topology. (Sumathi et al., 2015)

2.1.5.7.2. Fixed Speed Wind Turbine

Fixed-speed wind turbine operates at both a constant and constant frequency (Mittal et al., 2010). The wind turbine must be capable of providing inertial and primary frequency response. If the turbine achieves this capability, the technology can support the grid's frequency stability (Muljadi et al., 2013; Jung et al., 2017).

Three types of fixed-speed wind turbines can be distinguished based on the three power control methods, namely stall control (passive control), pitch control (active control), and active stall control (see Figure 2.13) (Letcher, 2017).

a) Fixed speed Wind Turbine based on Passive Stall Control

The passive stall control allows the wind turbine to be controlled by the stalled blade by limiting the rotational speed. This method makes the wind turbines operate at maximum efficiency under low and medium speed and high wind speed. Hence, wind turbines get protected from excessive wind speed. Passive stall control is cheaper than active stall control. However, it necessitates external accessories to start the wind turbine (Letcher, 2017).

b) Fixed speed Wind Turbine based on Active Stall Control

Active stall control refers to actively controlling a stall of the blade by pitching the blades in a direction contrary to a pitch-controlled wind turbine. This movement increases the rotor blades' angle to make the blades go into a deeper stall and a larger attack angle. This method has the advantage of being able to compensate for the variations in air density (Letcher, 2017).

The active controlling method has two operating modes, namely the power limitation and the pitch angle. In the power limitation, the output is regulated to the rated power when wind speed is between rated wind speed and shutdown wind speed. While the pitch control is adjusted to control the stall effect, the system gets a flat power curve (Letcher, 2017).

c) Fixed speed Wind Turbine based on Pitch Control

Pitch control is the most common method of controlling the aerodynamic power generated by a turbine for novel more giant wind turbines. The technique consists of turning the blades quickly either into or away from the wind to lower or higher the power output; the pitch angle is adjusted by a fraction of a degree each time to modify the wind speed, hence, keep a fixed power output. This control approach's drawback is the need for the rotor geometry to change, making the system more expensive than the previous control methods for fixed speed wind turbines (Letcher, 2017).

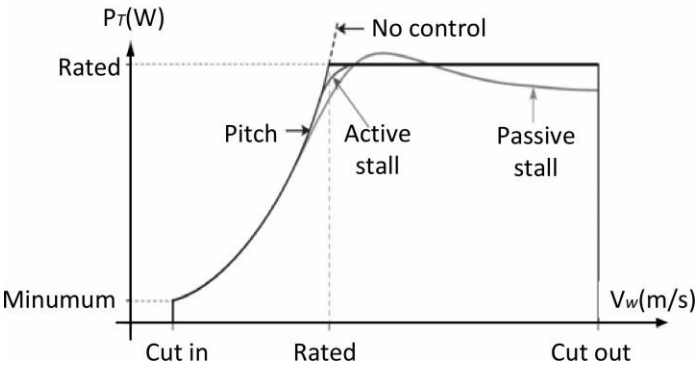

Figure 2.13: Fixed-speed wind turbine methods behaviour. (Zhao & Ding, 2018)

2.1.5.8. Aerodynamic of Wind Turbine

In a wind turbine, the wind flowing through the rotor blades at the speed rate is converted into mechanical energy (kinetic energy) (Zhao & Ding, 2018). The kinetic power can be expressed by Equation 2.3 as follows (Letcher, 2017; Abad et al., 2011):

$$P_t = \frac{1}{2}\rho v_0^{\,3} A$$

Equation 2.3

where P_t is the wind kinetic power, A is the swept area, ρ is the air density, v_0 is the wind velocity.

2.1.5.8.1. Power of the Wind Turbine

The power extracted by a wind turbine is given in Equation 2.4 (Abad et al., 2011; Sau-Bassols et al., 2016):

$$P(v, \lambda, \beta) = \frac{1}{2} C_p(\lambda, \beta) \rho \pi R^2 v^3$$

Equation 2.4

Where P is the extracted power, R is the radius of the rotor, ρ is the air density, v is the wind velocity, λ is the tip ratio, β is the pitch angle, and C_p is the wind power coefficient.

2.1.5.8.2. Wind Turbine Power Coefficient (C_p)

The wind power coefficient quantifies the wind turbine's efficiency (Letcher, 2017); it represents a fraction of the wind's power extracted by the rotor. Additionally, it evaluates the wind turbine performance. C_p is usually defined by the following equation (Manwell et al., 2009):

$$C_p(\lambda, \beta) = \frac{P_M}{P_V} = \frac{\text{Power of the wind turbine}}{\text{Power of the wind}}$$

Equation 2.5

The value of C_p varies according to the tip ratio and the pitch angle of the rotor.

2.1.5.8.3. Betz limit and Tip Ratio

The maximum value of the power coefficient that the wind turbines can extract is approximately 59.7%; this is known as the Betz limit (Sumathi et al., 2015). Furthermore, the tip-speed ratio λ (Whitby et al., 2014) is given by Equation 2.6 as:

$$\lambda = \frac{R\omega}{v}$$

Equation 2.6

where ω is the rotational speed of the turbine.

2.1.5.8.4. Wind Turbines Rotor Torque

Wind Turbine rotor torque is given by the fraction of the turbine power over the turbine rotational speed is provided by Equation 2.5 (Abad et al., 2011; Simani, 2015).

$$T_t = \frac{P}{\omega_r} = \frac{\rho\pi R^2 v^3}{2\omega} Cp(\lambda, \beta) = \frac{\rho\pi R^3 v^2}{2\lambda} Cp(\lambda, \beta)$$

Equation 2.7

where T_t is torque and ω_r the rotor speed.

2.1.5.9. Wind Turbines power output characteristics

2.1.5.9.1. Wind Turbines Power Curves

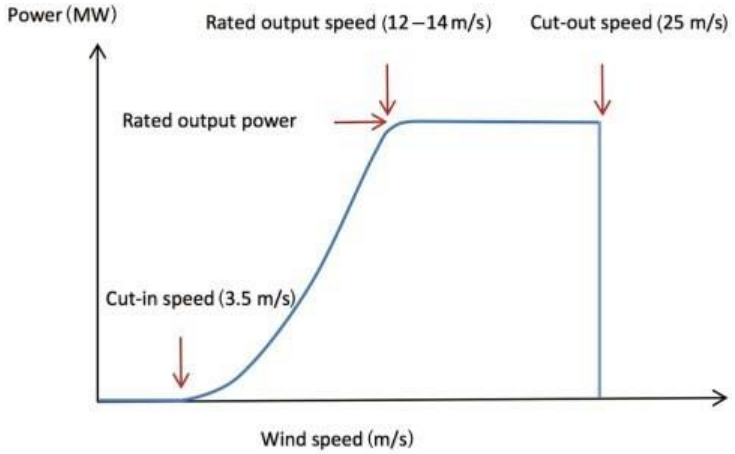

Figure 2.14: Typical Wind Turbine Power Speed. (Neill & Hashemi, 2018)

The wind power curve is a standard feature obtained from the manufacturer to predict the wind turbine output power (Zhao & Ding, 2018). It is depicted in Figure 2.14, where the cut-in speed defines the minimum wind speed to rotate the turbine. Generally, from zero to the cut-in speed, the wind turbine's power is near zero as there is still not enough kinetic energy to move the turbine. The rated speed refers to the minimum wind speed at which the turbine starts producing the rated power. Typical values of the rated speeds are between 13 and 16 m/s. Lastly, the cut-out speed is the maximum wind speed at which the turbine can produce power. Beyond this speed, the wind turbine is stopped (Sumathi et al., 2015). Common values of the cut-out speed are between 25 and 30 m/s (Neill & Hashemi, 2018).

2.1.5.9.2. Wind Power System Mathematical Model

The power curve defines the wind power, which establishes the relation between wind speed and power. This relation can be represented through Equation 2.6 (Dıaz-Dorado et al., 2013):

$$P_V = \begin{cases} p = 0 & V \le V_{cut-in} \\ q(V) & V \le V_{cut-in} \le V_{rated} \\ P_r & V_{rated} < V < V_{cut-off} \end{cases}$$

Equation 2.8

Where P_V is the electric power, V_{cut-in} is the cut-in wind speed, $V_{cut-off}$ is the cut-out wind speed in m/s, V_{rated} is the rated wind speed, $\mathrm{P_r}$ The rated power of the wind turbine and $\mathrm{q(v)}$ is the non-linear relationship between power electric and wind speed.

2.2. PWM Regenerative Rectifier and Controls

Power converters play a significant role in wind power conversion systems, as they can increase the dynamic, steady-state performance and improve the power quality (Chen et al., 2009). Power converters for wind turbines include rectifiers, inverters, and back-to-back converters. However, this study focuses only on rectifiers.

2.2.3. Rectifier

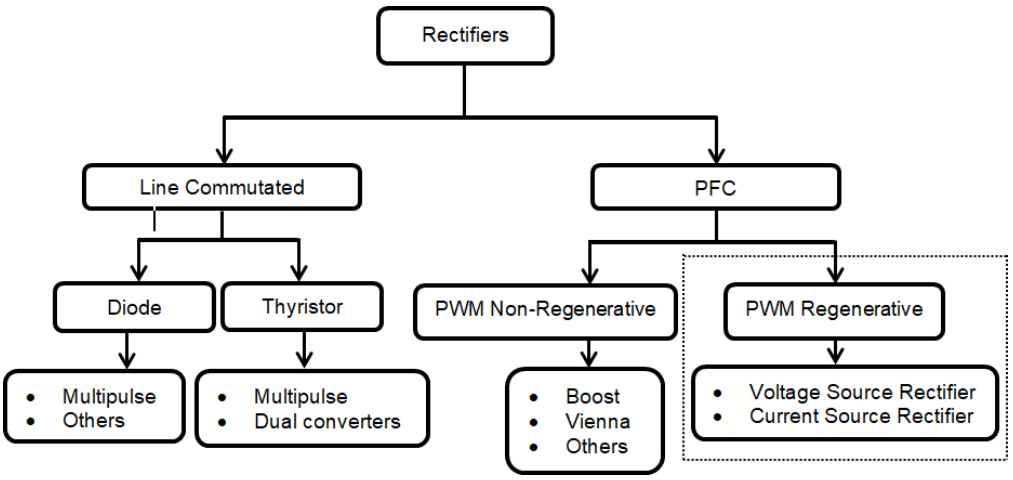

Figure 2.15: Rectifier Diagram adapted from. (Rodríguez et al., 2005)

Rectifiers are power converters that convert alternating current (AC) into direct current (DC). Rectifiers can be classified into two categories: Line Commuted and Power Factor Correction (PFC) rectifiers. Line commuted rectifiers can be further grouped into diodes and thyristor-based rectifiers (Figure 2.15). On the other hand, the PFC can be categorized into regenerative and non-regenerative rectifiers.

2.2.1.1. Line Commuted

Line Commuted converters are uncontrolled and convert stable AC voltages and currents into DC. There are based on diodes and thyristors and have the disadvantages of generating harmonics. Besides, the thyristor sometimes pollutes the line current when operating as a non-linear load (Gopalan, 2016).

2.2.1.2. PFC

The PFC rectifiers operate with a higher power factor as an active and reactive power combination (Gopalan, 2016). The non-regenerative rectifiers are unidirectional power flow, and the regenerative rectifiers are bidirectional power flow converters that in some cases operate in unidirectional mode (Blaabjerg, 2018).

2.2.1.2.1. PWM Non-Regenerative Rectifier

Non-regenerative rectifiers, including Boost and Vienna rectifiers, are merely utilised in systems in which the power flows only from the AC source to the DC load. For instance, the boost rectifiers usually are used in power generation to provide the desired magnitude voltage; this also converts a low-level DC voltage to a high-level DC voltage (Subhashini & Sankari, 2014).

2.2.1.2.1.1. PWM Three-phase Boost rectifier

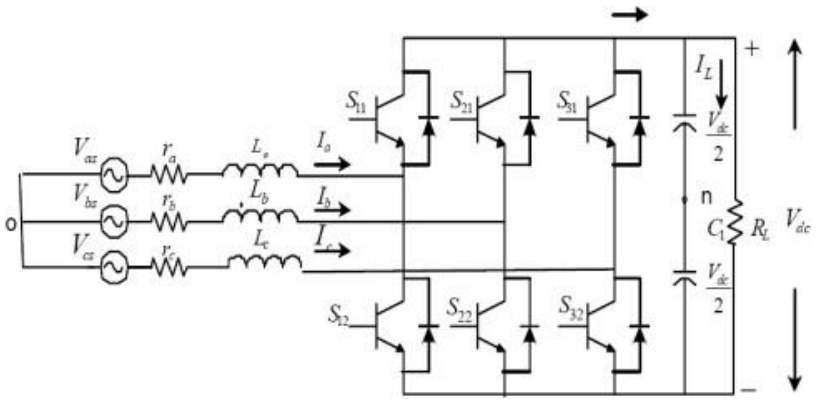

Figure 2.16: Schematic of boost Rectifier. (Rodríguez et al., 2005)

The three-phase boost rectifier consists of an asymmetric current drawing features, making it a preferable topology for high-power applications. Boost converters have been broadly employed since they provide low distortion line current with approximately unity power factor for several load conditions (Hassan & Abdullah, 2015). Their main disadvantage is the instability of the output voltage. A stable voltage can only be realised when the three-phase voltage supply is balanced. Otherwise, it can cause an abnormal second harmonic at the DC output voltage, generating third-order harmonic current to flow. A typical topology of a three-phase boost rectifier is depicted in Figure 2.16 (Subhashini & Sankari, 2014; Saher, 2012).

2.2.1.2.1.2. PWM Three-phase Vienna Rectifier

Vienna rectifiers are commonly used in high-power factor correction applications, including off-board electric (EV) chargers and telecom rectifiers. These rectifiers are low switch voltage devices, even though non-typical switches are required. On the

other hand, they need complex control design and sometimes unique semiconductor module fabrication (Saher, 2012).

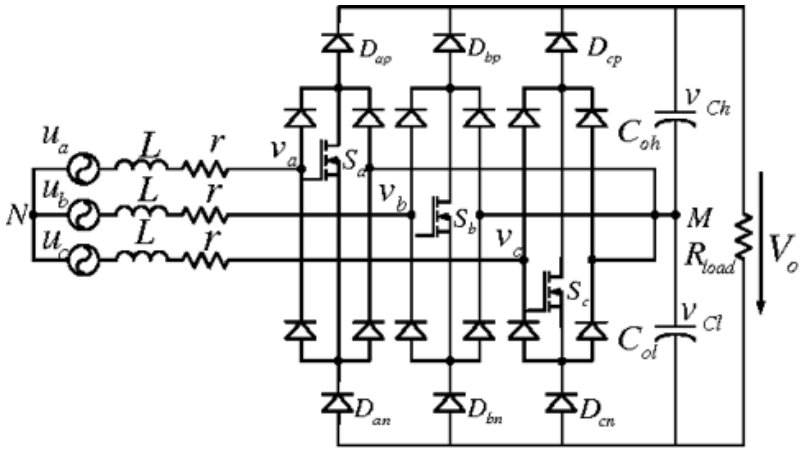

Figure 2.17: Schematic of Vienna Rectifier. (Rodríguez et al., 2005)

2.2.1.2.2. PWM Regenerative Rectifiers

Regenerative rectifiers operate in reversal mode; they are in most cases referred to as inverters since the topology implies the capability of transferring power in both directions, namely AC-to-DC and DC-to-AC as rectifiers and inverters, respectively. They are suitable for various applications with bidirectional power flow requirements, such as motor drives, high voltage direct current transmission systems (Khaburi & Nazempour, 2012), grid integration of wind turbines, and energy storage battery charging systems for electric vehicles. In these applications, the line side needs to transport energy back to the power generation.

Regenerative rectifiers are classified as Voltage Source Rectifier (VSR) or Current Source Rectifier (CSR) (Bhattacharya, 2014). A PWM regenerative rectifier enables controlling either the DC-link voltage or current by generating a DC-link voltage with a constant magnitude. It can operate in four quadrants with a high-power factor as a generator or load, depending on the quadrant. They present some advantages compared to Line Commuted rectifiers, due to a sinusoidal input current at unity power factor on the AC side. On top of a constant DC-link voltage and the bidirectional power flow (Trinh, Wang, Member, et al., 2017).

2.2.1.2.2.1. PWM Voltage Source Rectifier

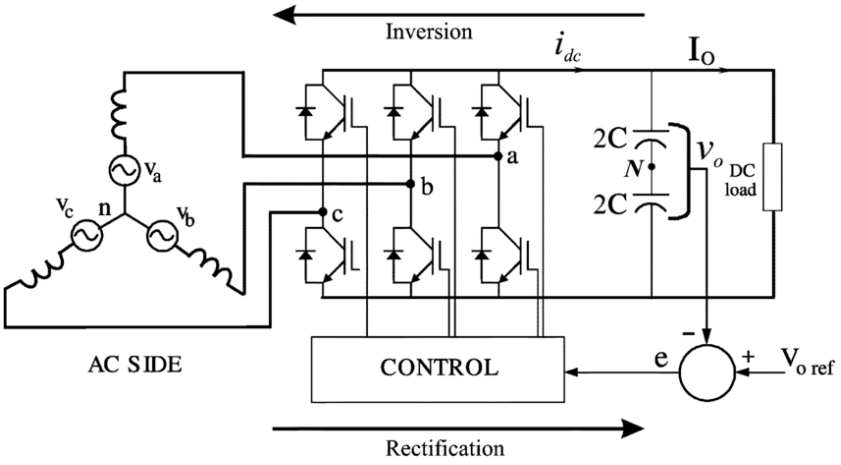

Figure 2.18: Schematic of Voltage Source Rectifier. (Rodríguez et al., 2005)

The VSR operates by keeping the load DC-link at an acceptable reference value, using a feedback control loop (see Figure 2.18). This reference must be high to keep the converter diodes blocked. Once this is achieved, the DC-link voltage is evaluated and compared with the reference. The error signal from the comparison is used to turn ON and OFF the valves of the VSR. Therefore, power can come or send back to the AC source based on the DC-link voltage value. If the DC load current is positive, the capacitor is discharging the mode, and the error signal is positive. Thus, the current flows from the AC to the DC side.

VSR topology allows the control of the magnitude, the phase angle, and output voltage frequency. In such converters, the DC side voltage always has one polarity, and the power reversal occurs into a reversal of DC polarity. On the other hand, the DC side voltage is supported by a capacitor. This capacitor can handle a constant charge or discharge current, which goes along with the switching sequence of the converter valves and shifts in the switching valves' phase angle with no change in the DC voltage (Chen & Jin, 2006; Navpreet et al., 2012). The input current and the DC-link voltage must be controlled to obtain a proper DC output power,; thus, the PF (power factor) is also controlled.

2.2.1.2.2.2. PWM Current Source Rectifier

A CSR (Figure 2.19) produces a controllable DC signal from an AC power input. Compared to VSR, the CSR has a continuous current and needs a filter capacitor at the input side (AC side) while requiring an inductance at the output side (DC side). This type of converter uses unidirectional switch devices like diode and thyristors.

Compared to the bidirectional devices (IGBT and MOSFET) for voltage source converters. CSRs have several advantages including (Blaabjerg, 2018):

- inherent short-circuit abilities,
- low differential voltage variation,
- direct output current controllability.

Such converters have been broadly utilised for DC voltage boost circuit in power supply and multiple-stage voltage conversion applications (DC-to-DC and DC-to-AC), superconducting energy storage systems, high-power metal industry (Zhao & Jiang, 2017), integration of offshore power generation systems to the grid, high voltage direct current and high-power drive systems (Wei et al., 2017).

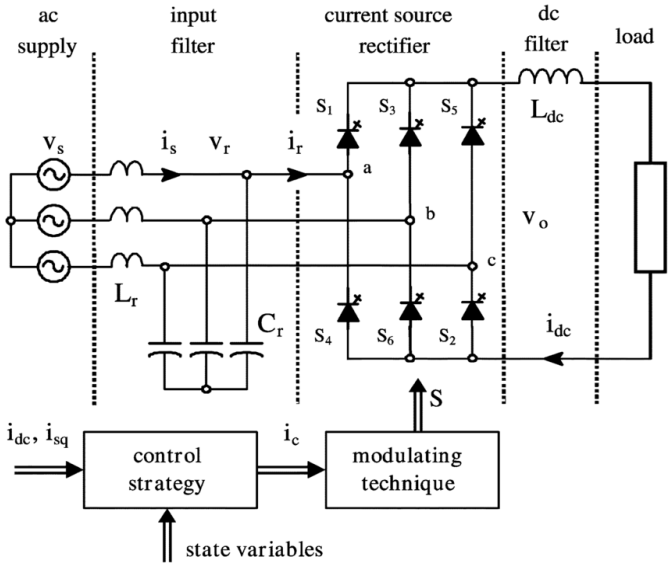

Figure 2.19: Three-phase current source rectifier layout. (Rodríguez et al., 2005)

2.2.1. Pulse Width Modulation (PWM) Techniques for Rectifiers

Pulse Width Modulation (PWM) creates sinusoidal currents and running sequences of pulse-width modulations to control power switches to produce outputs voltage and current for several types of loads and reduce harmonic contents in both voltage and current signals (Aktaibi et al., 2016). The requirements and optimisation standards employ PWM techniques. Each method's choice comes with the rectifiers' desired performance (Knapczykf & Pieńkowskif, 2006).

For rectifiers, PWM techniques aim to control the amplitude of the converter input PWM three-phase voltages' fundamental harmonics. The methods are generally categorized by various ranges of the linear operation, fixed switching frequency, and lower influence on generating the higher harmonics in currents (Knapczykf & Pieńkowskif, 2006; Kwasinski et al., 2003).

In general, PWM techniques for PWM rectifiers are as follows: hysteresis-band pulse-width modulation (HB-PWM), carrier-based sinusoidal pulse-width modulation (SPWM), space vector pulse-width modulation (SVPWM), and selective harmonic elimination (SHE) (Blaabjerg, 2018; Knapczykf & Pieńkowskif, 2006).

2.2.2.1. Hysteresis-Band Pulse Width Modulation (HB-PWM)

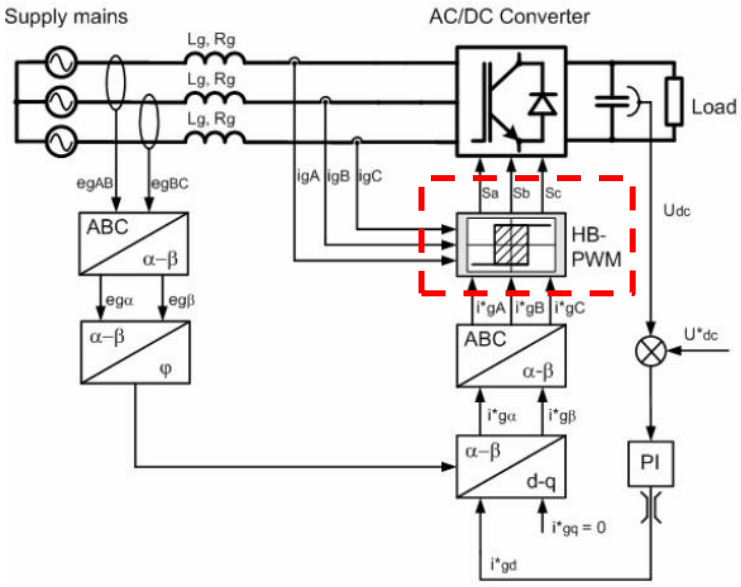

Figure 2.20: Hysteresis Band PWM technique. (Knapczykf & Pieńkowskif, 2006)

The HB-PWM is simple and provides a fast response and load-independent performance. However, the technique has some disadvantages, such as it has a variable switching frequency that requires high-bandwidth current sensors and sampling rate (Blaabjerg, 2018). The working principle of the HB-PWM is as follows: when the instantaneous value of the phase current becomes more significant than the reference value, the corresponding grid phase is connected to the negative node of the DC-link voltage, or else the grid phase is switched to the positive node in the DC-link (see Figure 2.20) (Knapczykf & Pieńkowskif, 2006). The best application of the hysteresis technique is found in the three-phase rectifier voltage. It has a lower ripple, which makes the use of the hysteresis technique a good choice when a high-bandwidth current sensor and sampling rate are in place (Blaabjerg, 2018).

2.2.2.2. Carrier-based sinusoidal pulse-width modulation (SPWM)

The sinusoidal Pulse Width Modulation technique uses a triangular carrier to generate the PWM pattern. The method was at the beginning developed for three-phase voltage source inverters (VSI); however, it was extended for three-phase current source rectifiers and in some cases for voltage source rectifiers (Rodríguez et al., 2005).

In voltage source rectifiers, to ensure that the rectifier performs well, the PWM pattern must produce enough PWM sinewave with the same frequency as the power source (input voltage). By modifying the PWM sinewave amplitude and its phase, the rectifier can be controlled to function in the following modes: leading power factor both rectifier and inverter and lagging power factor both rectifier and inverter (Rodríguez et al., 2005).

SPWM technique operating principle consists of comparing the converter voltage reference (trapezoidal modulation wave) with a carrier wave (Blaabjerg, 2018). Its application can be seen in voltage-oriented control (Figure 2.21). Compared to HB-PWM with the reference current signals, the SPWM technique provides the firing pulses on the converter voltage signals (Knapczykf & Pieńkowskif, 2006).

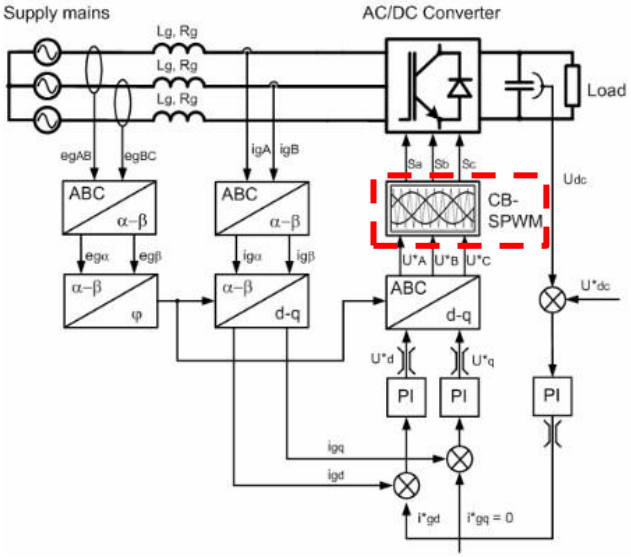

Figure 2.21. Voltage-oriented control with SPWM. (Knapczykf & Pieńkowskif, 2006)

2.2.2.3. Space Vector Pulse-Width Modulation (SVPWM)

SVPWM technique generates switching signals in rectifiers combined with voltage-oriented control (Jamma et al., 2016; Trinh, Wang & Choo, 2017). In such a method, the highest magnitude of the voltage that each vector can output varies in quantity to the DC-link voltage. As a result, when the DC-link voltage changes, the magnitude of the output voltage follows the same step (Bongiorno & Svensson, 2007; Jung et al., 2018; Hong et al., 2018). On the other hand, SVPWM offers a dynamic and robust way to eliminate input harmonics. Its benefits consist of increasing the output voltage fundamental component and provide a constant switching frequency (Riveros et al., 2019).

A typical SVPWM diagram is depicted in Figure 2.22, which refers to the steady-state vector. The six active conduction states in the hexagon (V1 to V6) are output voltage vectors from the converter AC-to-DC. Each vector is phase-shift by π $\frac{}{3}$ and their magnitude is proportional to the DC-link voltage of the converter $\frac{2VDC}{3}$. While V0 and V7 vectors are represented as zero voltage since there is no actual voltage output to the AC sideload. (Bongiorno & Svensson, 2007; Choe et al., 2016).

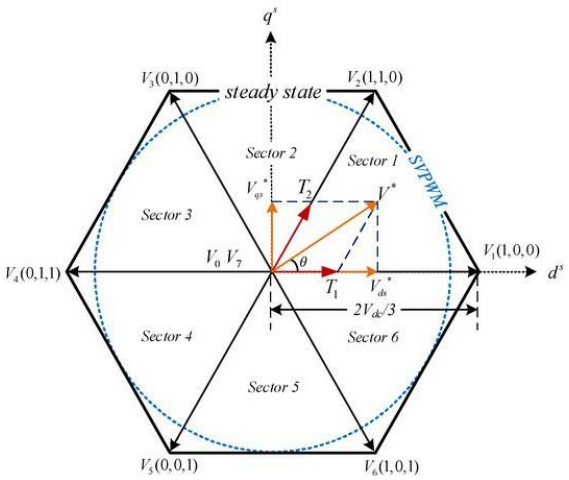

Figure 2.22: Space Vector steady state. (Hong et al., 2018)

Compared to other techniques, SVPWM solves the system instabilities generated by SPWM and HB-PWM. SVPWM has a characteristic of processing the entire complex voltage vector, whereas the hysteresis and sinusoidal technique process separately (Badr et al., 2015; Kumar & Sundareswaran, 2015).

2.2.2.4. Selective Harmonics Elimination (SHE)

SHE usually deals with the gating design of the current source rectifier. The technique defines the gating signal to eliminate some predefined harmonics and control the input current's fundamental amplitude (Rodríguez et al., 2005). The low switching frequency is always susceptible to produce low-order harmonics that cause notable line current distortion due to their converter topology's filter circuit (Zhang et al., 2014). Therefore, to reduce disturbances, the SHE technique is adopted in the high-power PWM current converters (such as high-power current source converters based drive) due to its superior harmonic performance at low switching frequency (Blaabjerg, 2018).

For example, since the CSR (Figure 2.23 and Figure 2.24) topologies implies capacitors at the input side to support the commutation of switching devices that create a capacitive-inductance filter with the grid line impedance filter reactor (Zhang et al., 2014). The selective harmonic elimination is the better choice of a modulation technique to reduce the line disturbances' potential problem.

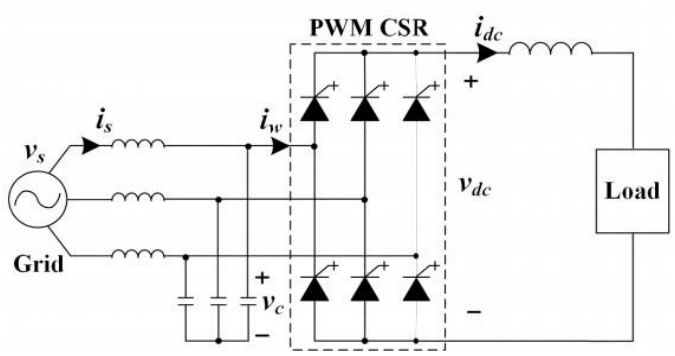

Figure 2.23: PWM CSR topology. (Zhang et al., 2014)

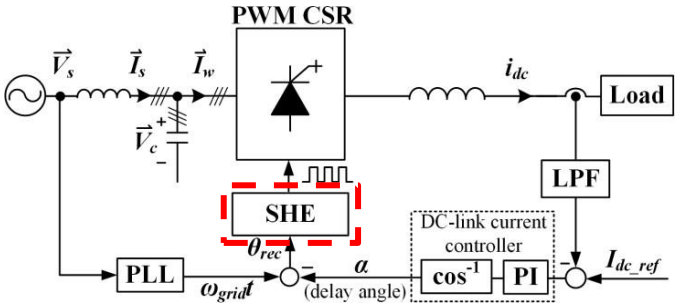

Figure 2.24: High-power current source rectifier control diagram. (Zhang et al., 2014**)**

2.2.2. Control Approaches for PWM Regenerative Rectifier

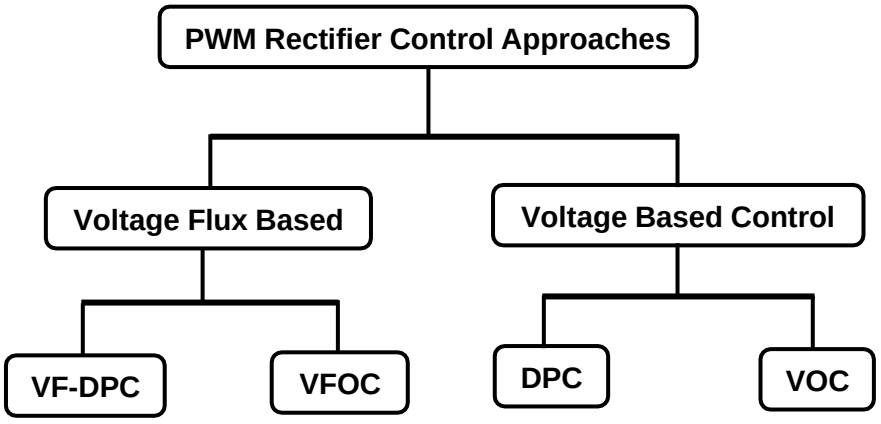

Figure 2.25: Controls Strategies for PWM Rectifiers adapted from. (Malinowski et al., 2003)

Control approaches for PWM regenerative rectifiers can be classified into two main categories, namely, voltage oriented based control and virtual-flux based control (Harshada, 2016). Both types are distributed into two subcategories (Figure 2.25). The referred subcategories are Virtual-Flux Based Control: Virtual Flux-Direct Power Control (VF-DPC) and Virtual Flux-Oriented Control (VFOC); Voltage Oriented Based

Control: Voltage-Oriented Control (VOC) and Voltage-Based Direct Power Control (DPC) (Hassan & Abdullah, 2015; Harshada, 2016).

Although these control strategies may achieve the same goals for high power factor and near-sinusoidal input current waveforms, some of their principles differ. (Hassan & Abdullah, 2015; Sanjuan, 2010).

2.2.3.1. Virtual Flux Direct Power Control (VF-DPC)

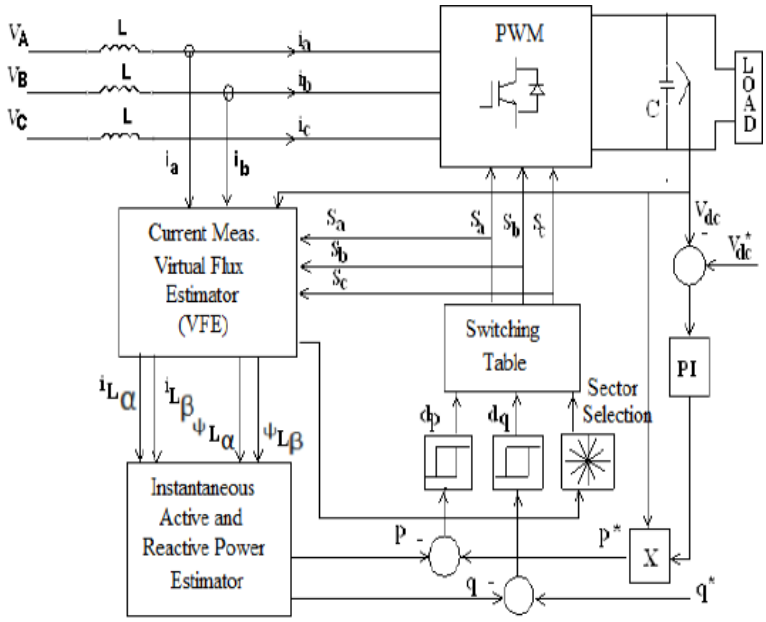

Figure 2.26: Virtual Flux Direct Power Control. (Harshada, 2016)

Virtual Flux is utilised for instantaneous active and reactive power estimation. It can combine direct power control with the input value estimation method for three-phase rectifiers (Yusoff et al., 2017). Unlike other control methods, VF-DPC does not require line voltage sensors. It does not need to coordinate transformation, voltage modulators, current regulation loops, and decoupling between control of the active and reactive components (Sanjuan, 2010). The strategy can quickly implement the unbalance and distorted line voltage compensation to find the sinusoidal line currents (Khaburi & Nazempour, 2012). Its algorithm is more superficial and has better dynamic performance than voltage-oriented control (Malinowski et al., 2001). The primary virtual flux direct power control topology is depicted in Figure 2.26, where V_{dc} is the measured DC-link voltage, S_a, S_b, S_c are the switch states of the PWM rectifier, i_a, i_b, i_c are the measured line currents, and L is the inductance between the generator and PWM rectifier (Malinowski et al., 2001).

2.2.3.2. Virtual Flux Oriented Control (VFOC)

The Virtual flux strategy improves the rectifier control under non-ideal line voltage conditions (Sanjuan, 2010). VFOC is a sensorless voltage method, and it is based on VOC (Figure 2.27). However, the AC side voltage is computed using virtual flux, the converter switching states, and the DC voltage (Kakkar et al., 2019). This method also has some disadvantages, such as the coupling occurring between active and reactive components and requires decoupling solutions.

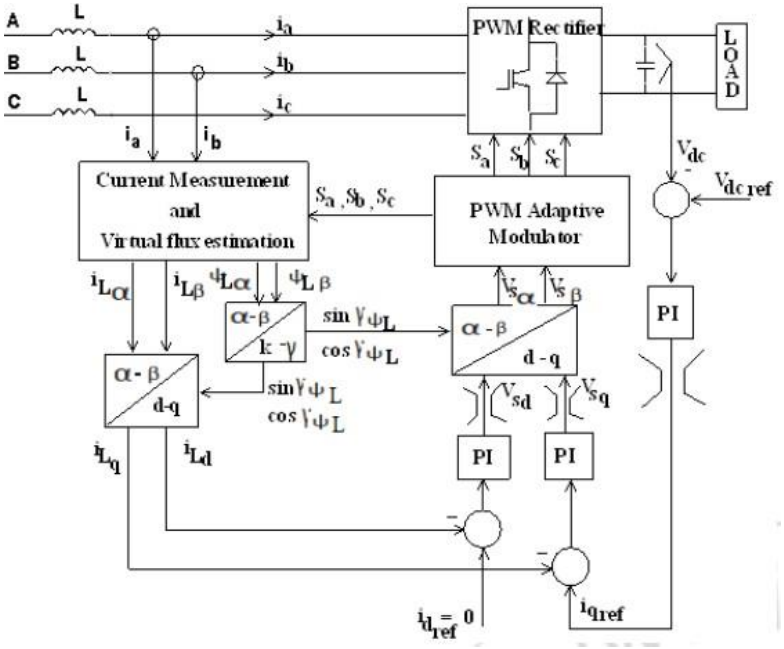

Figure 2.27: Virtual flux oriented control. (Harshada, 2016)

2.2.3.3. Voltage Oriented Control (VOC)

The schematic in Figure 2.28 shows the three-phase PWM rectifier topology based on VOC strategy using sensors to size the line voltage. A characteristic feature of this current controller is represented in two coordinate transformations. The first one is the stationary α-β, and the second one is the synchronous rotating d-q reference systems. In the topology, the measured values are converted to the equivalent stationary α-β. The output is then transformed into a rotating coordinate system in a block α-β or d-q (Malinowski, 2001).

The VOC has high dynamic and static performance through an internal current control loop. Hence, the implementation relies on the current control strategy (Marian et al., 2002; Kondylis et al., 2017). In VOC, the input line current can be oriented by the line voltage vector. And this last is found through the measurement by using either sensor or estimation. Its line voltage vector is also used as a reference, and it aligns the d-axis in the synchronous reference frame. The VOC diagram in Figure 2.28 also shows that

the d-axis (active power) component of the line current is proportional to the active power,. In contrast, the q-axis (reactive power) component is proportional to reactive power.

In this approach, the only way to achieve a unity power factor is to set the reactive component of the current reference to zero. In contrast, the active component of current reference is found using the traditional proportional integrative controller (PI), which presents the result through a comparison of the DC-link voltage at the output with the reference voltage set by the load requirements (Zhang & Qu, 2015; Harshada, 2016).

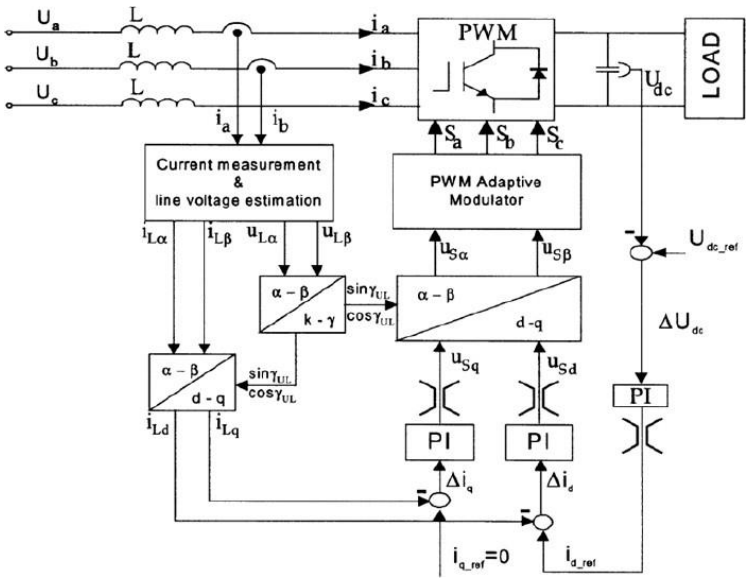

Figure 2.28: Typical block diagram for Voltage-Oriented Control. (Sanjuan, 2010)

2.2.3.4. Voltage based Direct Power Control (DPC)

The DPC (Figure 2.29) is based on the direct control of active and reactive power control loops (Sanjuan, 2010). There is no need of the current internal control loop and the PWM modulator block as its converter switching states are set through the pattern value based on the direct errors between the commanded and estimated values of active and reactive power (Hassan & Abdullah, 2015).

The DPC power estimation depends on the line voltage. Hence, it has some disadvantages, such as the need for high sample frequency because of the constant estimated value change. It requires high inductance value due to the switching frequency instability, which causes difficulties in designing an input filter (Sanjuan, 2010).

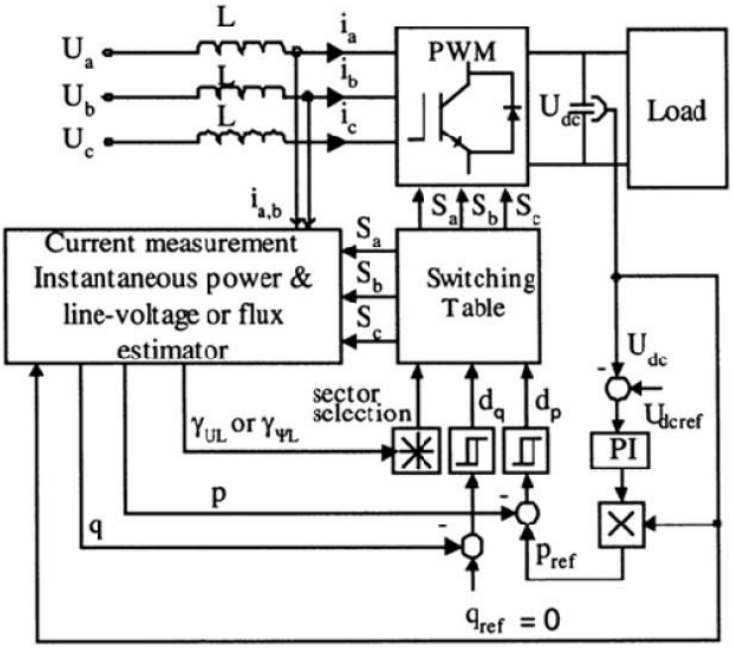

Figure 2.29: Direct Power Control block diagram. (Sanjuan, 2010)

Table 2.3 shows some advantages and disadvantages of the PWM regenerative rectifier control approaches.

Table 2.3: Advantages and disadvantages of PWM rectifiers control strategies. (Malinowski et al., 2003)

Technique	Advantages	Disadvantages
VOC	• Fixed switching frequency- (easier design of the input filter), • Advanced PWM strategies can be used, • Cheaper A/D converters, • No sensitivity to line inductance variation.	• Coordinate transformation and decoupling between active and reactive power components required, • Complex algorithm • Input power factor lower than that for V-DPC.
VFOC	• Fixed switching frequency, • Advanced PWM strategies can be used, • Cheaper A/D converters, • No sensitivity to line inductance variation.	• Coordinate transformation and decoupling between active and reactive components is required; • Complex algorithm Input power factor than that of VF-DPC.
DPC	• No separate PWM voltage modulation block, • No current regulation loops, • No coordinate transformation, • Good dynamic performance, • Decoupling active and reactive power control, • Instantaneous variables with all harmonic components are estimated (improvement of the power factor and efficiency).	• High values of the inductance and sampling frequency are needed, • Power and voltage estimation should be avoided at the moment of switching (if yields high errors), • Variable switching frequency, • Fast microprocessor and A/D converters required.
VF-DPC	• Simple and noise-resistant power estimation algorithm, easy implement in DPC, • Low THD of line currents at a distorted and unbalanced supply voltage; Good dynamic performance, • Decoupled active and reactive power control.	• Variable switching, • Fast microprocessors and A/D converters required.

CHAPTER THREE

SYSTEM MODELLING

This chapter deals with the modelling of a PMSG wind generator connected to a PWM regenerative rectifier supplying a DC load. The components modelled in this chapter include a PMSG and a PWM rectifier. Figure 3.1 shows the main elements of the system.

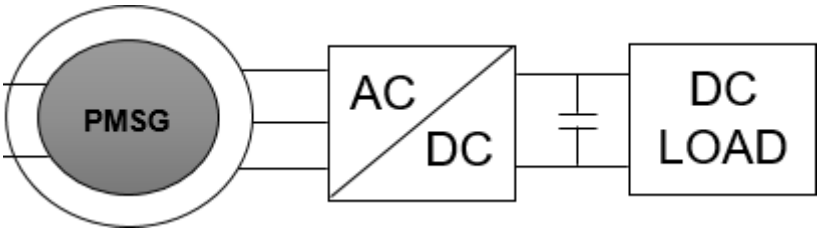

Figure 3.1: System design.

3.1. Modelling of Permanent Magnet Synchronous Wind Generator

A PMSG offers a high-efficiency power conversion from mechanical to electrical power. In this type of generator, the excitation field is given by a permanent magnet rather than a coil. It is referred to as a synchronous generator because the rotor and the magnetic field rotate at the same speed. A shaft generates the magnetic field mounted permanent magnet mechanism, and the current is induced into the stationary armature (Binder & Schneider, 2005). Two types of PMSGs can be distinguished, namely the salient rotor and round rotor. This study considers a round rotor generator.

The nominal magnetic flux Φ_{nom} in a round rotor PMSG is expressed as (Caixeta et al., 2014):

$$\Phi_{nom} = \frac{\sqrt{6}\,V_{nom}}{3\omega_{nom}}$$

Equation 3.1

Where V_{nom} is the nominal voltage, ω_{nom} is the angular velocity of the generator, and Φ is the magnetic flux.

The linkage magnetic flux Φ can be evaluated using Equation 3.2 as follows:

$$\Phi = \phi_{pu} \times \Phi_{nom}$$

Equation 3.2

Where ϕ_{pu} is the magnetic flux per unit value, and Φ_{nom} is the total flux of the magnet.

The nominal power P_{nom} of a round rotor PMSG is given the following equation:

$$P_{nom} = \sqrt{3} V_{nom} I_{nom} cos\varphi$$

Equation 3.3

Where V_{nom}, I_{nom} and $cos\varphi$ are the nominal voltage, current, and power factor, respectively.

The nominal impedance Z_{nom} of a round rotor PMSG is determined as follows:

$$Z_{nom} = \frac{\sqrt{3} V_{nom}}{3 I_{nom}}$$

Equation 3.4

The stator resistance R_s is defined by the following equation:

$$R_s = R_{s_{pu}} Z_{nom}$$

Equation 3.5

Where $R_{s_{pu}}$ is the resistance per unit value, and Z_{nom} is the nominal impedance.

The nominal inductance L_{nom} of a round rotor PMSG is determined as follows:

$$L_{nom} = \frac{Z_{nom}}{\omega_{nom}}$$

Equation 3.6

Where ω_{nom} is the angular velocity.

The inductance of a round rotor PMSG L_{dq} in dq0 frame can be expressed as follows:

$$L_{dq} = L_{dq\_pu} L_{nom}$$

Equation 3.7

Where L_{dq_pu} is the inductance per unit value.

The moment of inertia J of a round rotor PMSG is given by equation 3.8 as follows (Wang et al., 2015):

$$J = \frac{2 {N_p}^2 H P_{nom}}{{\omega_{nom}}^2}$$

Equation 3.8

Where N_p is the number of pole pairs and H is the inertia constant.

The parameters used in the modelling of the permanent magnet synchronous wind generator are given in Table 3.1.

Table 3.1: Wind generator modelling parameter.

Parameters	Values
P_{nom}	1.53 MW
V_{nom}	953 V
$R_{s_{pu}}$	0.027
R_s	0.006Ω
L_{dq_pu}	0.5131
L_{dq}	0.000395 H
ϕ_{pu}	1.18842
Φ_{nom}	2.4768 Wb
Φ	1.48 Wb
J	35000 kgm^2
N_p	48
ω_{nom}	6.542 rad/sec
H	5.005

3.2. Modelling of the aerodynamic

The power P extracted by the wind turbine is determined by the following equations:

$$P_M = \frac{1}{2} C_p(\lambda, \beta) \rho \pi R^2 v_{rated}^3$$

Equation 3.9

Where R is the radius of the rotor, ρ is the air density, v_{rated} is the wind velocity, λ is the tip ratio, β is the blade pitch angle, and C_p is the wind power coefficient (Sau-Bassols et al., 2016).

The wind turbine coefficient is expressed by the following equation (Caixeta et al., 2014):

$$C_p(\lambda, \beta) = \frac{P_M}{P_v}$$

Equation 3.10

Where P_v is the power of the wind.

The equation of the torque T_t is expressed as (Hannachi & Benhamed, 2017):

$$T_t = \frac{\rho \pi R^3 v^2 C_p}{2\lambda}$$

Equation 3.11

The optimal rotational speed of the wind turbine generator Ω_R is given in equation 3.12 as follows:

$$\Omega_R = \frac{\lambda_{optimal}\, v_{wind}}{R}$$

Equation 3.12

Where v_{wind} is the turbine speed, $\lambda_{optimal}$ is the optimal tip speed ratio (Wang et al., 2014).

The aerodynamics parameters of the wind turbine used in this study are given in Table 3.2.

Table 3.2:The aerodynamics of wind turbine parameters.

Parameters	**Value**
P_M	1.6 MW
T_t	$1.4.10^5$ Nm
$C_p(\lambda, \beta)$	0.34
ρ	1.12
R	33.05 m
v_{rated}	13.36 m/s
Ω_R	0.4
$\lambda_{optimal}$	10.5

3.3. Modelling of PWM regenerative rectifier

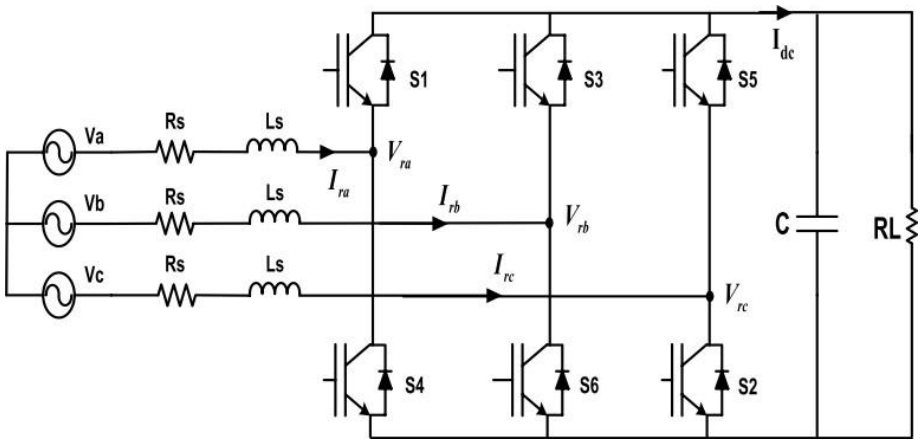

Figure 3.2: Two-level rectifier VSC topology. (Acikgoz et al., 2016)

The layout of a PWM three-phase regenerative rectifier is depicted in Figure 3.2. It is a voltage source rectifier consisting of a line inductance on the AC side (L_s, R_s), six individual IGBT switches, and a DC-link capacitor C on the DC side. The rectifier received AC power from a balanced three-phase voltage source (V_a, V_b, V_c) and the current supplied are I_{ra}, I_{rb} and I_{rc}. The DC output of the rectifier provides a current I_{dc} to a load RL.

The voltage of a three-phase voltage source PWM rectifier in abc coordinates is given as follows (Brito et al., 2015; Acikgoz et al., 2016):

$$\begin{matrix} L_s \frac{dI_{ra}}{dt} \\ L_s \frac{dI_{rb}}{dt} \\ L_s \frac{dI_{rc}}{dt} \\ \left[L_s \frac{dI_{uc}}{dt}\right] \end{matrix} = \begin{bmatrix} -R_s & 0 & 0 & 0 \\ 0 & -R_s & 0 & 0 \\ 0 & 0 & -R_s & 0 \\ S_a & S_b & S_c & -1 \end{bmatrix} \begin{bmatrix} I_{ra} \\ I_{rb} \\ I_{rc} \\ I_L \end{bmatrix} + \begin{bmatrix} V_a - V_{ra} \\ V_b - V_{rb} \\ V_c - V_{rc} \\ 0 \end{bmatrix}$$

Equation 3.13

Where V_{ra}, V_{rb} and V_{rc} are the rectifier input voltages expressed as a function of switching devices, and S_a, S_b and S_c are the switching functions, either 0 (switch is off) or 1 (switch on).

And:

$$\begin{cases} V_a = V_m sin\theta \\ V_b = V_m sin\left(\theta - \frac{2\pi}{3}\right) \\ V_c = V_m sin\left(\theta + \frac{2\pi}{3}\right) \end{cases}$$

Equation 3.14

Using Clake's transformation, the dynamic model of the PWM rectifier is given as follows:

$$\begin{bmatrix} V_\alpha \\ V_\beta \end{bmatrix} = L_s \begin{bmatrix} \frac{dI_\alpha}{dt} \\ \frac{dI_\beta}{dt} \end{bmatrix} + \begin{bmatrix} R_s & 0 \\ 0 & R_s \end{bmatrix} \begin{bmatrix} I_\alpha \\ I_\beta \end{bmatrix} + \begin{bmatrix} V_{r\alpha} \\ V_{r\beta} \end{bmatrix}$$

Equation 3.15

Where V_α and V_β, $V_{r\alpha}$ and $V_{r\beta}$, and I_α and I_β are the voltage V_a, V_b and V_c, the voltage V_{ra}, V_{rb} and V_{rc}, and the current I_{ra}, I_{rb} and I_{rc} in $\alpha\beta$ frame, respectively.

In the same manner, using Park's transformation, the model PWM rectifier equation is expressed as:

$$\begin{bmatrix} V_d \\ V_q \end{bmatrix} = L_s \begin{bmatrix} \frac{dI_d}{dt} \\ \frac{dI_q}{dt} \end{bmatrix} + \begin{bmatrix} R_s & -\omega L_s \\ \omega L_s & R_s \end{bmatrix} \begin{bmatrix} I_d \\ I_q \end{bmatrix} + \begin{bmatrix} V_{rd} \\ V_{rq} \end{bmatrix}$$

Equation 3.16

Where V_d and V_q, V_{rd} and V_{rq}, and I_d and I_q are the voltage V_a, V_b and V_c, the voltage V_{ra}, V_{rb} and V_{rc}, and the current I_{ra}, I_{rb} and I_{rc} in dq frame respectively, and $\theta = \omega t$ is the angle between the d-axis and q-axis.

By transforming Equation 3.16 into d-q rotating reference frame, the Equation will become (Chen & Jin, 2006).

$$\begin{cases} V_d = L_s \frac{di_d}{dt} + \omega L_s i_q + u_d \\ 0 = L_s \frac{di_q}{dt} - \omega L_s i_d + u_q \end{cases}$$

Equation 3.16

Where the resistance value is neglected as it is very small and $V_q = 0$.

3.4. Modelling of Line Inductance

The inductance has a significant role in the rectifier operation. It generates an induced voltage that makes the voltage source rectifier operate in boost mode and allows the DC-link voltage to be higher than the magnitude of the input voltage blocking the diodes for the system's proper operation. Besides, the inductance also operates as a filter to reduce the current ripple and reduces the rectifier's operation range at the same time (Chen & Jin, 2006). The voltage drop across the inductance controls the current, and this voltage is controlled by the rectifier, although its highest value is limited by the DC-link voltage (Marian et al., 2002). The inductance can be determined using equation 3.17 as follows (Wang et al., 2013):

$$L_s \geq \frac{(2V_{dc} - 3E_m)E_m T_s}{2V_{dc}\Delta I_{max}}$$

Equation 3.17

Where ΔI_{max} is the maximum ripple current generally chosen as 20% of the maximum current, E_m is the peak voltage of the AC generator, and T_s is the sampling period.

3.5. Modelling of DC-link voltage

A proper operation of the rectifier depends on the minimum DC-link voltage, which is generally determined by the peak of line to line voltage given in equation 3.18 as follows (Marian et al., 2002):

$$V_{DC-min} > \sqrt{2}\,\sqrt{3}\,V_{LN(rms)} = \sqrt{3}\,E_m$$

Equation 3.18

Where V_{DC-min} is the minimum DC-Link and $V_{LN(rms)}$ is the line to ground voltage. However, in general, the DC-link voltage depends on the PWM technique, in this study, the minimum DC-link voltage is determined using equation 3.20 expressed as: Considering the maximum reference voltage as $\frac{VDC}{2}$, the Equation 3.19, will be expressed as follows (Sanjuan, 2010):

$$V_{LN(Peak)} = \frac{V_{DC}}{2}$$
$$\frac{\sqrt{2}}{\sqrt{3}} V_{LL(rms)} = \frac{V_{DC}}{2}$$
$$V_{DC-min} > 2V_{LN(peak)} = \frac{2\sqrt{2}}{\sqrt{3}}\ V_{LN(rms)} = 1.663\,V_{LL(rms)}$$

Equation 3.19

However, in this study, the DC link voltage is considered as not complying with Equation 3.19.

The DC-link capacitor can be determined using the following equation:

$$C_{DC} = \frac{P}{2\pi f V_{DC} \Delta V_{DC}}$$

Equation 3.20

Where ΔV_{DC} is the maximum ripple DC voltage, and it is usually 5% of the supply voltage, V_{DC} is the DC bus voltage, P is the active power, and f is the generator frequency.

Table 3.3: PWM regenerative rectifier modelling parameter

Parameters	Values
V_{dc}	1150 Volts
V_{LL}	953 Volts
R_s	0.005 Ω
C_{DC}	0.0885 F
L_s	4.14x10^{-3} H

3.6. Control scheme

The control scheme adopted in this study is the voltage-oriented control strategy depicted in Figure 3.3. The system has a fast dynamic response and consists of controlling the output DC voltage through a double loop structure of the current. The outer loop is a DC-link voltage control producing the inner current references.

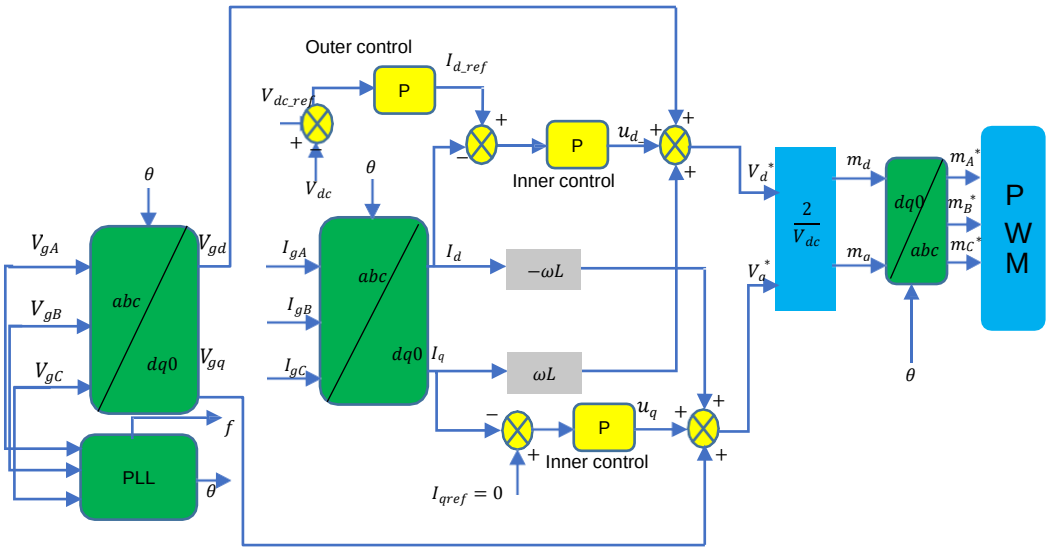

Figure 3.3: PWM rectifier control scheme. (Esmaeilian et al., 2014; Qi et al., 2014)

3.6.1. Outer loop control

The outer loop control maintains the DC-link voltage value close to a set DC reference voltage, which must be higher than the generator peak voltage to keep the converter's diode blocked. When this condition is satisfied, the DC-link voltage is measured and compared to the set DC reference. The error obtained from the comparison is used to generate the reference i_d^* current for the current loop through a PI controller (Chen & Jin, 2006). The transfer function of the outer loop controller is given as:

$$TF_v = k_{pv} + \frac{k_{pv}}{sT_{iv}}$$

Equation 3.21

Where the tuning parameters can be estimated as follows (Teodorescu et al., 2011):

$$\begin{cases} k_{pv} = 0.12\,\dfrac{C_{dc}}{T_s} \\ T_{iv} = 17T_s \end{cases}$$

Equation 3.22

Where k_{pv} is the proportional gain, T_{iv} the time integrator in the outer voltage loop, T_s is the sampling period given by:

$$T_s = \frac{1}{f_s}$$

Equation 3.23

3.6.2. Inner Loop Control

In the inner loop, the current i_d and i_q obtained through the dq0 transformation of the generator current (I_a, I_b and I_c) are compared respectively with the i_{d_ref} generated at the outer loop and i_{q_ref} which is set to zero (Pashaei & Aydemir, 2014). The transfer function of the inner loop controller is given as (Esmaeilian et al., 2014):

$$TF_i = k_{pi} + \frac{k_{pi}}{sT_{ii}}$$

Equation 3.24

Where k_{pi} and T_{ii} are estimated using the following equation (Teodorescu et al., 2011):

$$\begin{cases} k_{pi} = \dfrac{L_s}{3T_s} \\ T_{ii} = \dfrac{L_s}{R_s} \end{cases}$$

Equation 3.25

Where k_{pi} is the proportional gain and T_{ii} is the integration time constant of the inner loop control.

Table 3.4 gives the tuning parameters of both the outer and the inner loop controls.

Table 3.4: Rectifier control design parameters

Control loop parameters	
Outer loop	
k_{pv}	49.35
T_{iv}	2.81 mill seconds
Inner loop	
k_{pi}	0.3497
T_{ii}	64.13 milliseconds

3.6.3. Modulation Control

The modulation signals m_d^* and m_q^* are used to generate the PWM signals to drive the rectifier switches based on the following equation (Esmaeilian et al., 2014):

$$\begin{cases} m_d^* = \dfrac{2}{V_d}(V_{gd} + L_S\omega I_q + u_d) \\ m_q^* = \dfrac{2}{V_{dc}}(V_{gq} - L_S\omega I_d + u_q) \end{cases}$$

Equation 3.26

Where V_{gd} and V_{gq} are the disturbances from input power transmission, u_d and u_q are the current errors output signals.

3.6.4. Modelling of Phase Locked Loop (PLL)

The Phase-Locked Loop (PLL) is used in this study to generate the phase angle for the transformation. A typical PLL circuit consists of the phase detector, the loop filter, and the voltage-controlled oscillator (Behera & Thakur, 2016). The closed-loop transfer function of a PLL (Figure 3.5) is given by the following equation (Timbus et al., 2005):

$$G_{PLL}(S) = \frac{\theta^*}{\theta} = \frac{K_1 s + K_2}{s^2 + K_1 s + K_2}$$

Equation 3.27

Where K_1 is the PI loop filter proportional and K_2 is the proportional corresponding integral gain.

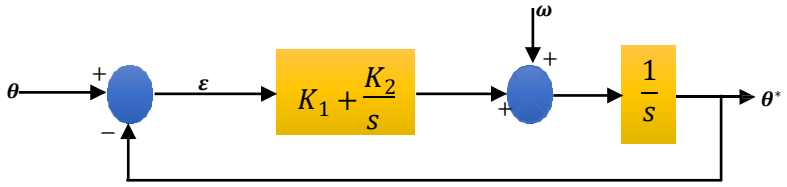

Figure 3.4: Small-signal model. (Behera & Thakur, 2016)

The parameters K_1 and K_2 of a PLL can be evaluated using the following expression (Teodorescu et al., 2011):

$$\begin{cases} \omega_{n-PLL} = \sqrt{K_2} \\ \xi_{PLL} = \dfrac{K_1}{2\sqrt{K_2}} \end{cases}$$

Equation 3.28

Where ω_{n-PLL} is the natural frequency and ξ_{PLL} is the damping ratio.
Table 3.6 provides the determined values of K_1 and K_2.

Table 3.5:Phased Locked loop parameters.

PLL parameters	
K_1	1
K_2	356

CHAPTER FOUR

SIMULATION RESULT AND DISCUSSION

4.1. Introduction

A simulation was carried out to analyse the model's performance depicted in Figure 4.1 using the Matlab/Simulink environment for a simulation time of 20 seconds based on parameters presented from Table 3.1 to Table 3.5. The system's operation is such that depending on the available wind resources, the wind generator produces AC power at a constant wind velocity of about 13 m/s. The wind generator has a power rating of 1.53 MW with a phase to phase voltage of 953 V at 50 Hz. The power obtained at the wind generator's output terminals is rectified to feed a DC load connected at the output terminals of the rectifier. The rectifier's output power delivers DC power of a magnitude of 1.26 MW at 1150 V; hence, the rectifier efficiency is around 82 %. Three types of loads are considered to evaluate the rectifier's performance, namely an R load, an RL, and an RC load. The control approach used to regulate the rectifier's output parameters is based on the closed-loop voltage-oriented strategy shown in Figure 4.2. The control method is expected to maintain the DC output voltage as close to the adopted reference DC voltage of 1150 Volts through proportional-Integral controllers. The control strategy includes two control loops, namely the outer and the inner control loops. In this case, the outer control loop is the DC-link voltage control, aims to generate the inner current in dq0 reference (Figure 4.2). Whereas the inner control loop uses the error between the dq0 reference current generated by the outer control loop and the system currents. The error is then used in the inner PI controller to produce the modulation signal in the dq0 frame. Lastly, the output of the inner control loop in dq0 is transformed back to abc frame to obtain the modulation in the abc frame to generate the Pulse Width Modulation signals to drive the rectifier.

The simulation results are presented in three sections: the AC, control scheme, and DC side results. The AC section focuses on the PMSG voltage, current, active and reactive power, and the current, active, and reactive power voltage. The control scheme discusses the obtained PWM signals, whereas the DC side deals with the DC-link voltage and voltage, current, and power at the load side.

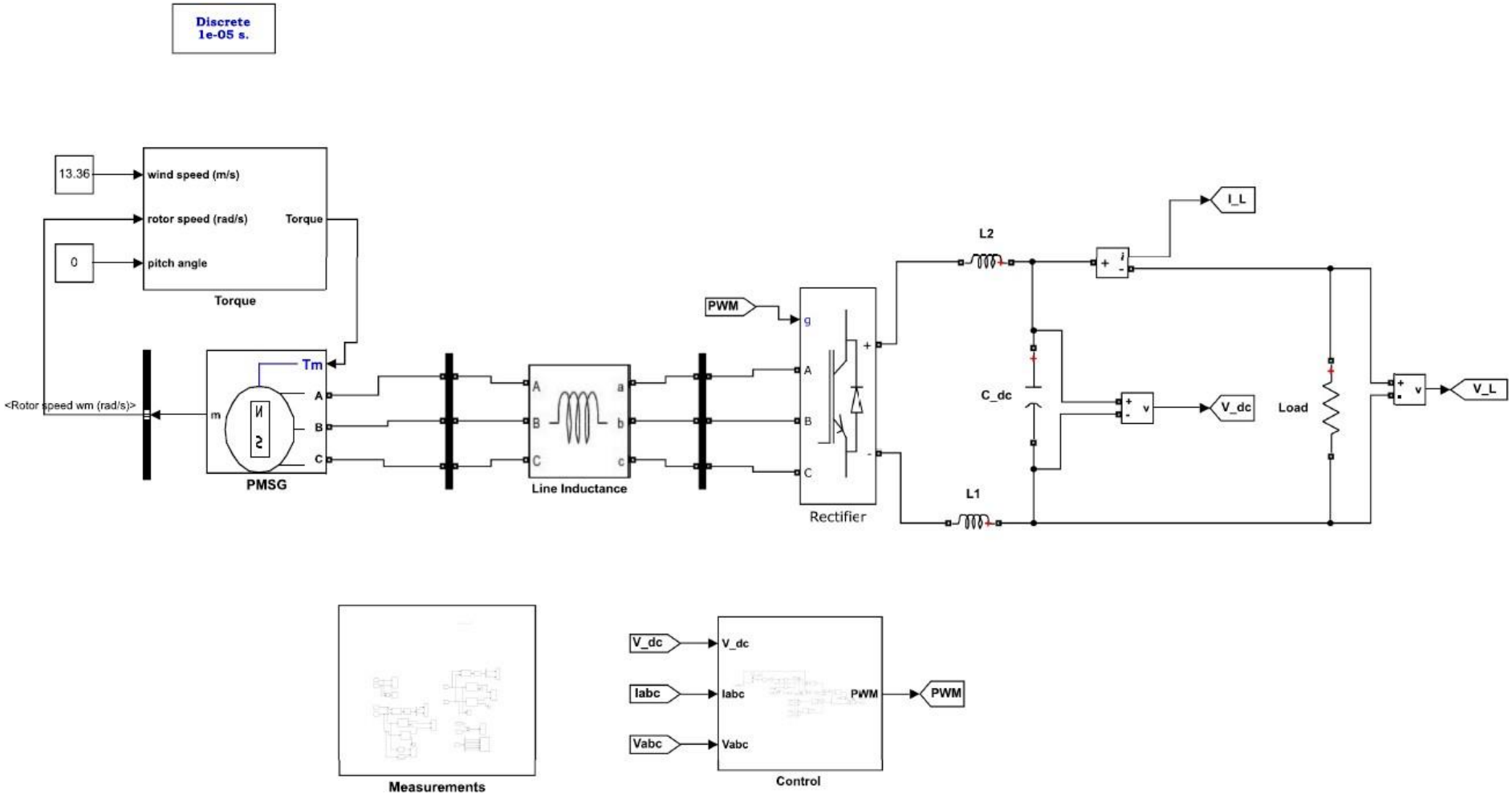

Figure 4.1: Permanent Magnet Synchronous Wind Generator connected to a PWM rectifier.

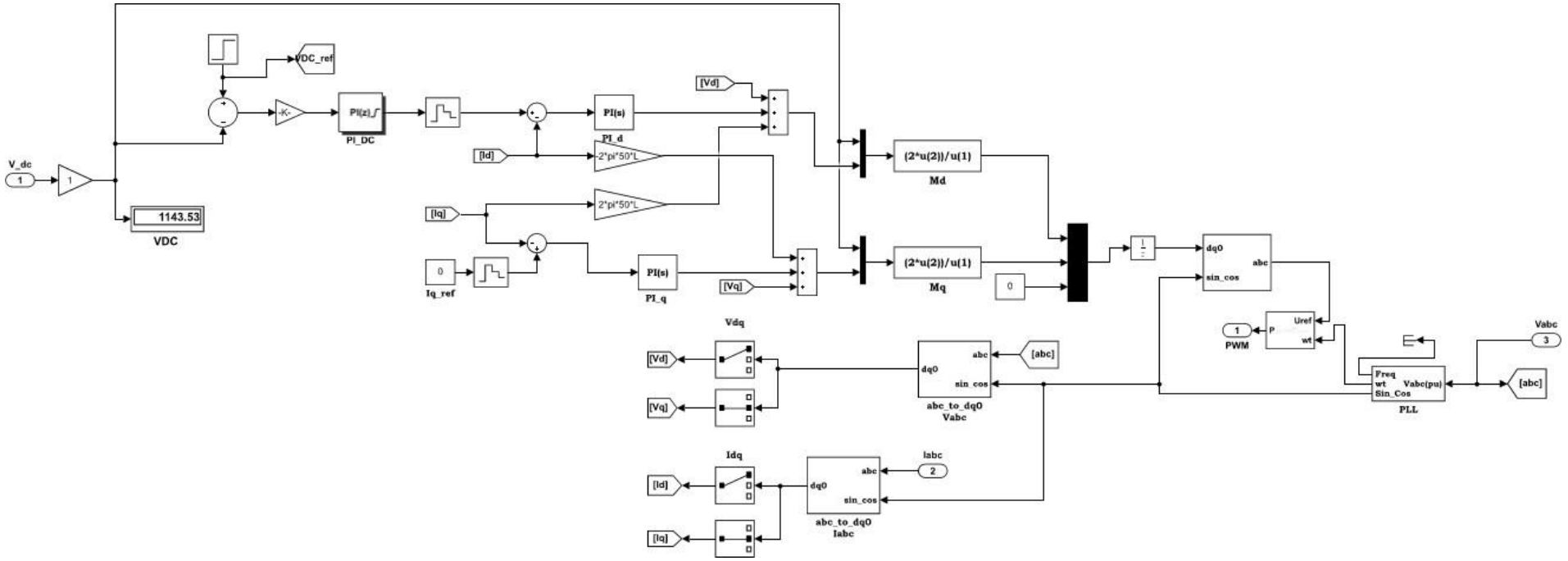

Figure 4.2: Voltage-Oriented Control Approach.

4.2. Results of the AC side

For a rated wind velocity of about 13 m/s, the wind generator's active and reactive power obtained from the simulation are shown in Figure 4.3. The average active power value is around 1.5 MW (Figure 4.3a), while the reactive power is 403 kW (Figure 4.3b). Between 0 and 3 seconds, the simulation results display an overshoot and undershoot for the active and reactive power signals, respectively, as the system did not reach its stability yet. However, after 3 seconds, it can be seen both signals gain their stability.

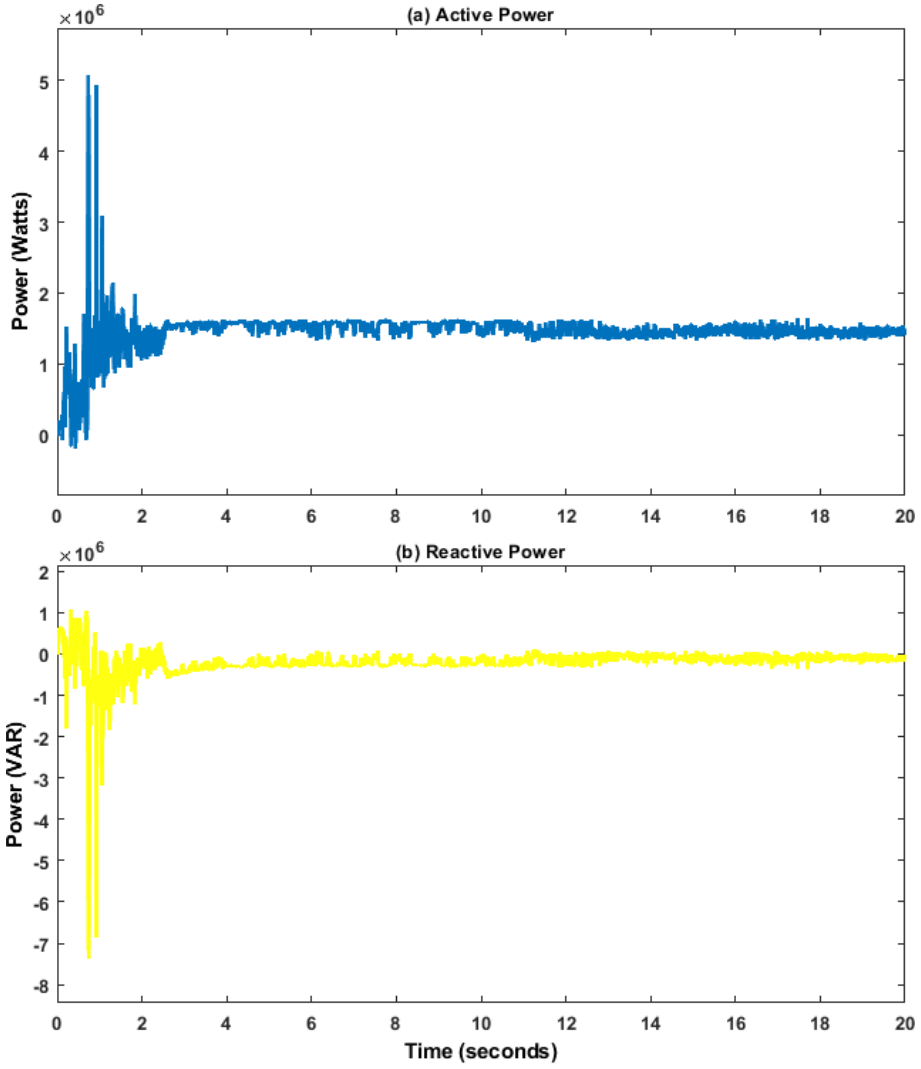

Figure 4.3: (a) Active Power and (b) Reactive power of the wind generator.

The phase to ground voltage and the phase current at the wind generator's output terminals are depicted in Figure 4.4. The RMS voltage value is around 549 V (Figure 4.4a), while the RMS of the phase to phase voltage is approximately 951 Volts. On the other hand, this generator's phase current is about 1082 Amps (Figure 4.4b). Both signals exhibit harmonics higher than the adopted system frequency of 50 Hz as shown in Figure 4.5.

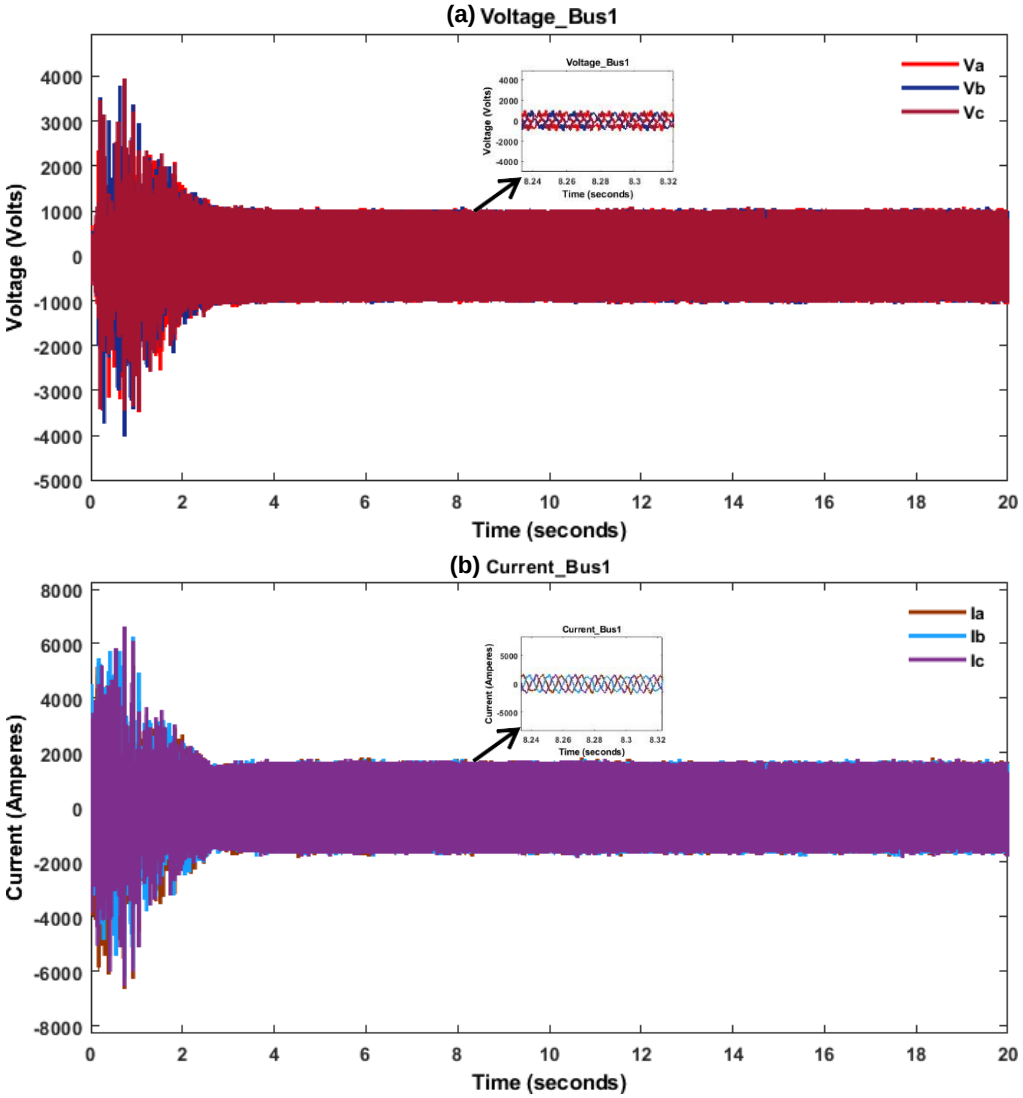

Figure 4.4: Voltage and (b) current curves of the wind generator

The phase to ground voltage wave is characterised by a Total Harmonics Distortion of 141.38% (Figure 4.5a), whereas the phase current signal shows a Total Harmonics distortion of 13.54% (Figure 4.5b).

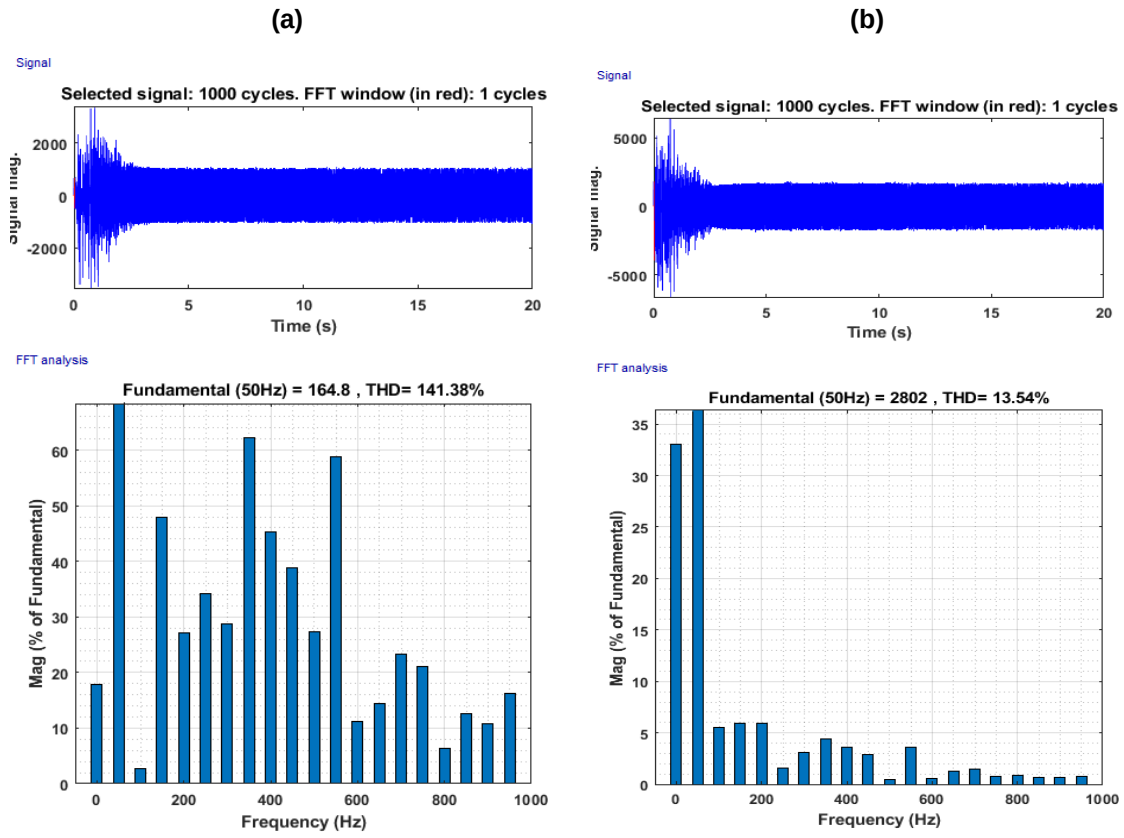

Figure 4.5: Voltage and (b) Current Total Harmonics Distortion.

4.3. Control scheme

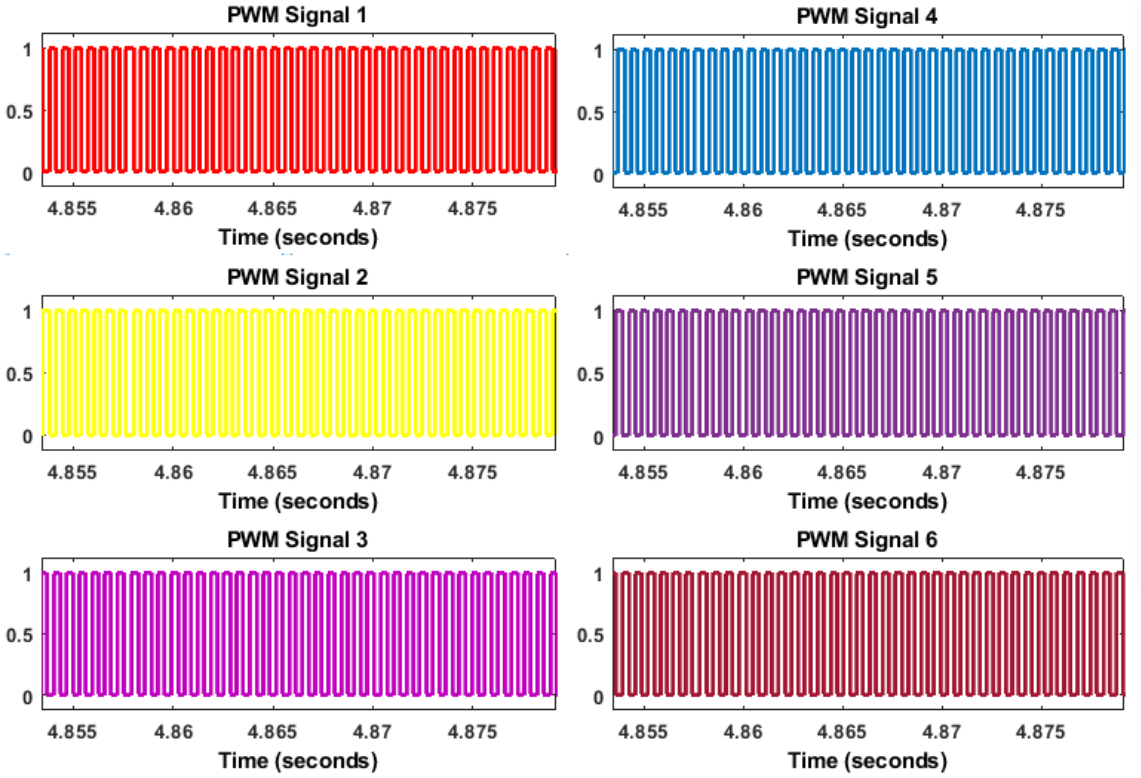

Figure 4.6: Generated PWM signals.

The adopted control technique maintains the DC output voltage closed to the reference DC voltage of 1150 V. The DC-link voltage control generates the current in the dq0 frame, while the generated current control produces the modulation signal in the dq0 frame. The modulation signals in the dq0 frame are then transformed into abc frame to generate six Pulse Width Modulation signals shown in Figure 4.6 to drive the rectifier.

4.4 Results of the DC side

The DC side results consist of comparing the DC voltage of the rectifier against the DC reference voltage and assessing the rectifier's performance when its output is connected terminal to an R load, RL load, and RC load.

4.4.1. DC voltage versus DC reference voltage

Figure 4.7 compares the DC voltage and the DC reference voltage used in the control loop. The reference voltage is set to 1150 V, and at a steady-state, both the DC voltage and the DC reference voltage are approximately equal. The DC voltage has a rise time of about 2.599 seconds, required for the voltage to rise from 0 to 100 % of its final value. Furthermore, the overshoot and undershoot at the start of the signal are 0.505 % and 2 %, respectively.

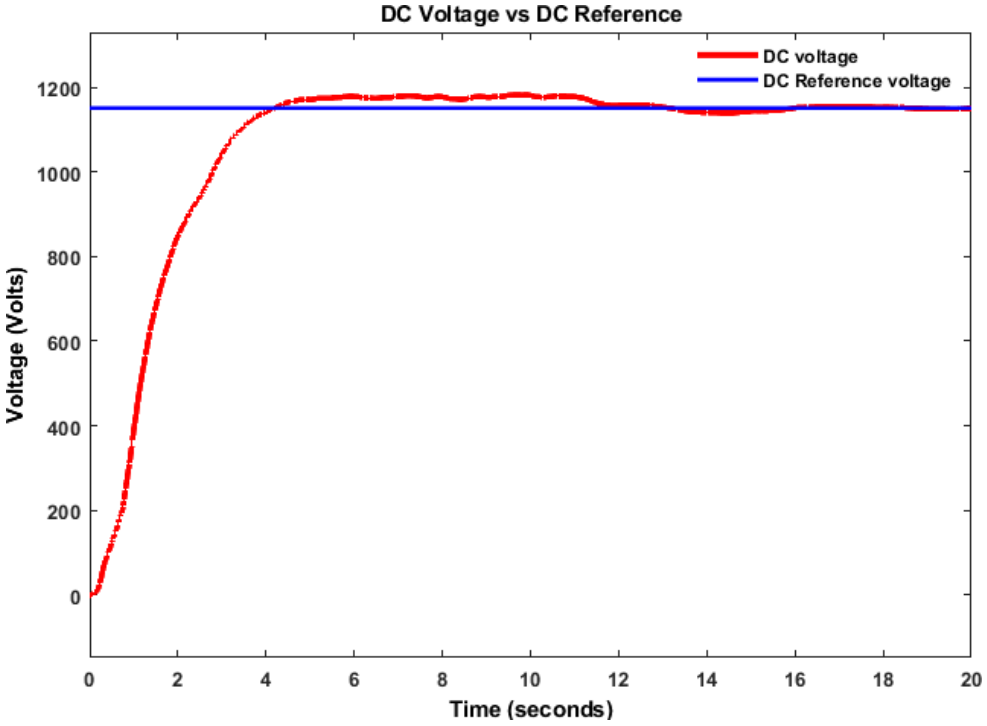

Figure 4.7: DC Voltage versus DC Reference voltage

4.4.2. Case 1

This case considers a purely resistive load of impedance equals to 1.02 Ω, which corresponds approximately to 1.29 MW (Figure 4.9). The load voltage and current are shown in Figure 4.8; the value of the voltage is 1146 V (Figure 4.8a), while the current is 1097 Amps (Figure 4.8b).

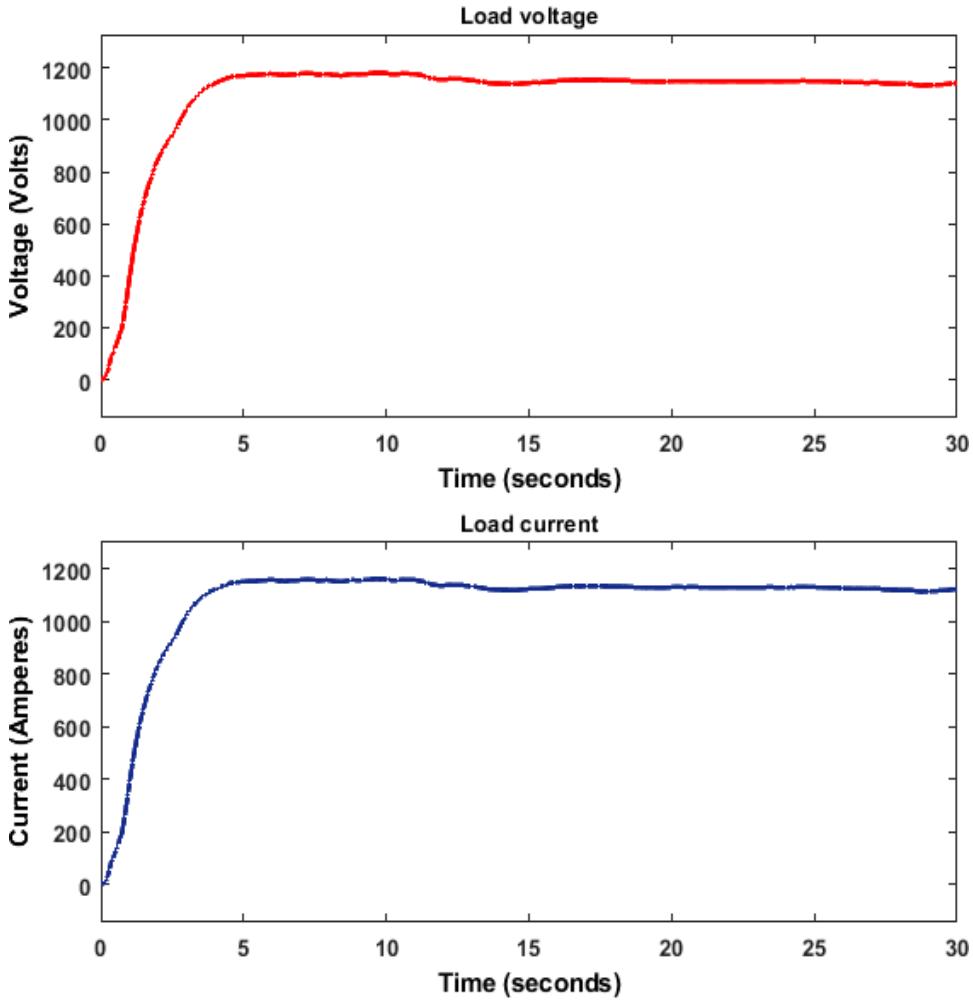

Figure 4.8: Voltage and Current of an R load.

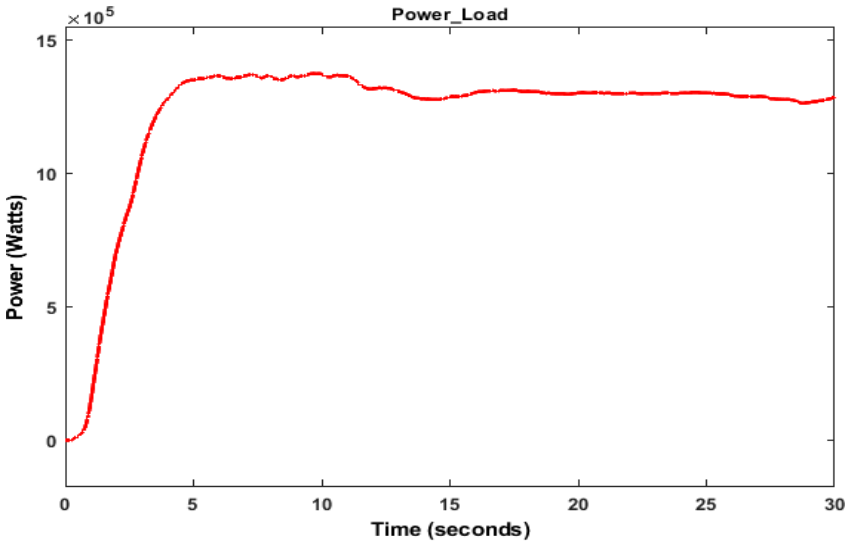

Figure 4.9: Power of a R load

4.4.3. Case 2

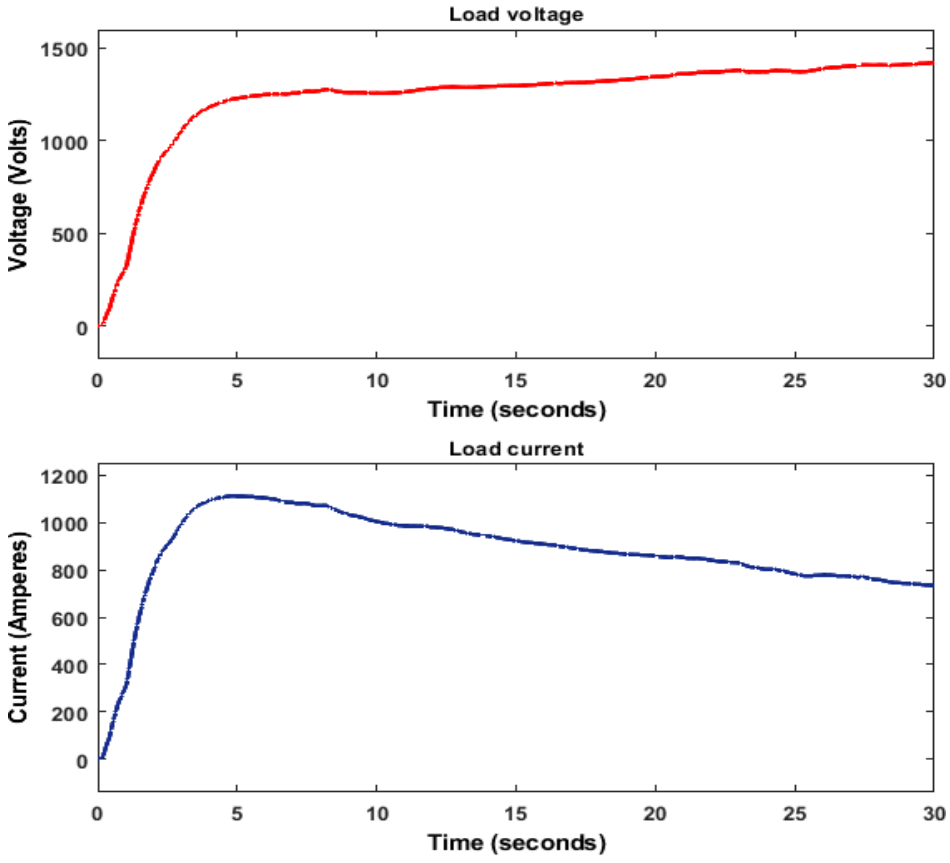

Figure 4.10: Voltage and Current of a RC load.

This case considers a load of impedance equals to 1.02 ohm comprising a resistance of 1.02 ohm and a capacitor bank of 4.13 Farad connected in series. The resulting active power is 1.29 MW. The load voltage and current are shown in Figure 4.10; the voltage increases to 1265 V due to the capacitor's presence (Figure 4.10a). The

obtained voltage shows an increase of about 100 V than the reference voltage of 1150V, while the current drops to 900 Amps (Figure 4.10b).

The power supplied to the load shown in Figure 4.11 displays a peak value of approximately 1.48 MW at around 5 seconds. Thereafter, it drops to reach a stable value of 1.15 MW, which is about 14 kW, lesser than the active power obtained when connecting the rectifier to a purely resistive load.

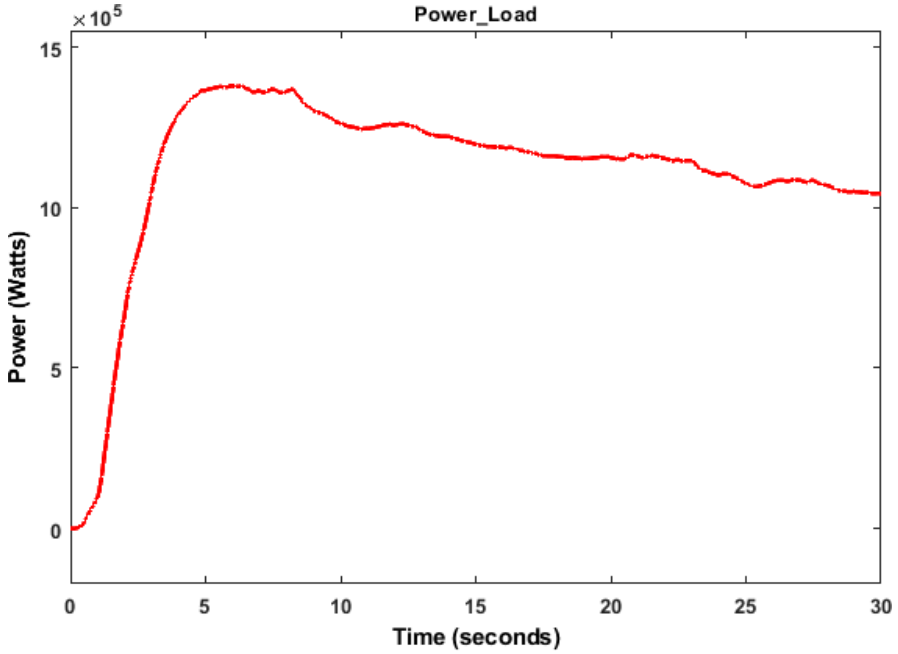

Figure 4.11: Power of an RC load

4.4.4. Case 3

The last case considers a load of impedance equals to 1.02 Ω, consisting of resistance of 1.02 Ω and inductance of 1 Henry connected in series. The voltage and current that supply the load are shown in Figure 4.11. From the beginning of the simulation, it can be observed that the voltage signal has oscillations until it reaches its stability and settles at 1105 V (Figure 4.11a), while the current shows less oscillation until it gets 1162 Amps (Figure 4.11b).

The resulting power measured at the load side is shown in Figure 4.12; this power oscillates between 0 seconds to about 16 seconds until it gets to apparent stability around 17 seconds (Figure 4.12). The measured power value is 1.207 MW, slightly lower than the power in case of a resistive load.

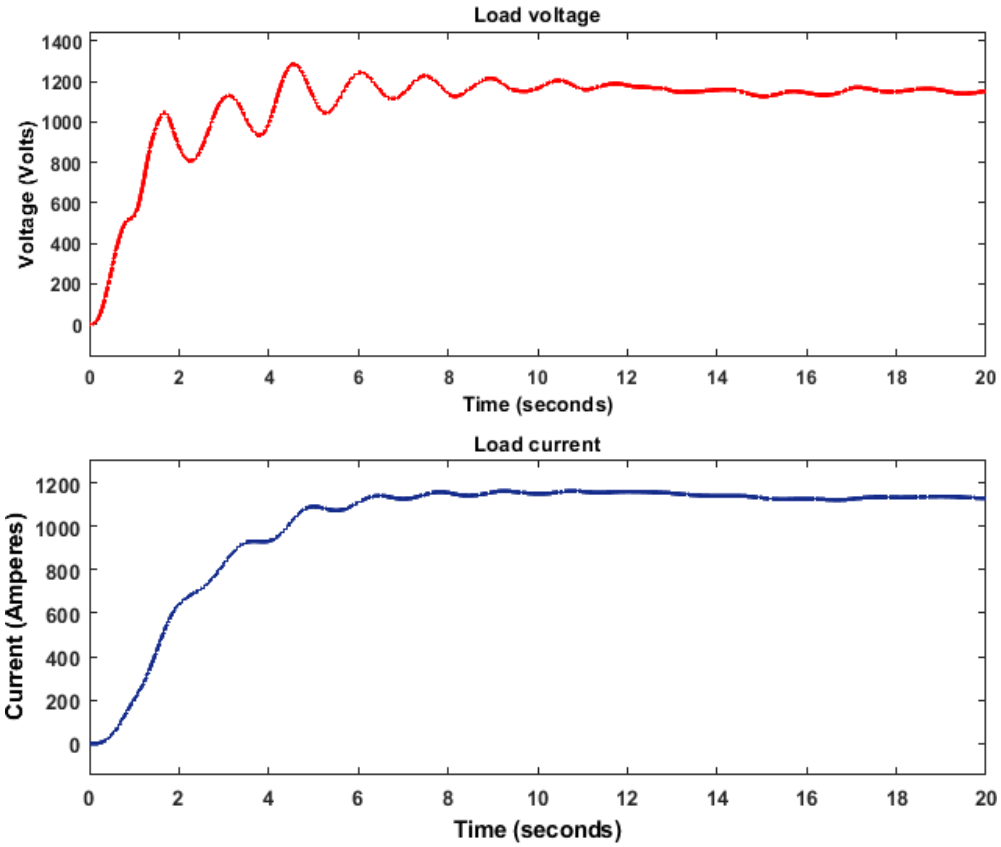

Figure 4.12:Voltage and Current of a RL load.

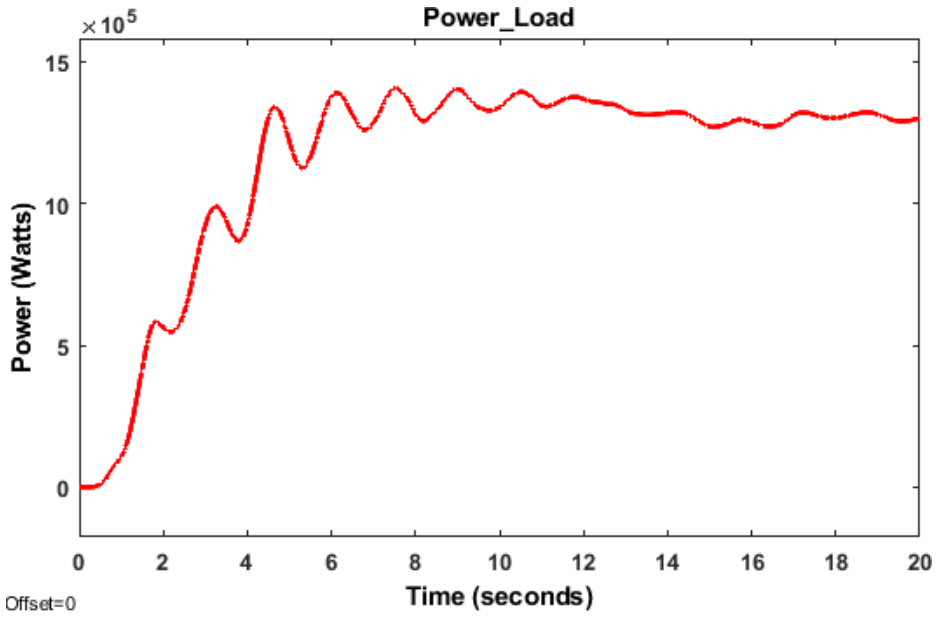

Figure 4.13: Power supplied to RL load.

CHAPTER FIVE

5. CONCLUSION AND FURTHER RESEARCH

5.1. Conclusion

When using renewable technologies such as photovoltaic panels or wind generators, the principal issue is their dependency on weather conditions, which cause their power outputs to be unreliable. In general, power converters are used as interfaces between these generators and the loads to condition the power before supplying it to a load. For wind power systems, three primary power converters can be employed, namely AC to DC converters (rectifiers) or DC to AC converters (inverters) or a combination of both types (back-to-back converters). AC to DC converters can be off line commutated type or power factor correction types. The power factor correction rectifiers consist of PWM regenerative and PWM non-regenerative rectifiers. This study aimed to develop a control scheme for a three-phase PWM regenerative rectifier receiving AC power from a 1.53 MW permanent magnet synchronous wind generator at a line voltage of 953 V. The rectifier delivered 1.26 MW at a DC voltage of 1150 V to a DC load connected to its output terminals. The control system scheme adopted in this study was based on a voltage-oriented control strategy. The modelling and simulation were carried out using Matlab/Simulink environment. Three types of loads, namely R, RL, and RC loads, were considered to evaluate the designed controller's performance. The results showed a good performance of the designed controller as the output voltage could be maintained close to the set reference value. At the same time, the rectifier delivered 1.26 MW to the load.

The research was divided into five chapters to achieve the aim of this study. Apart from the introductive and conclusive chapters, the rest of the study was summarised follows:

Chapter two was dedicated to the literature review on renewable power technologies and wind power generation. Furthermore, a section on PWM regenerative rectifiers and their control was also considered.

Chapter three covered the system description as well as the modelling of components involved in the system. A section referred to the modelling of the control system was also part of this chapter, which was carried out the modelling of PI controllers of the inner and outer control loops and the modelling of the phase-locked loop.

Chapter four focussed on presenting the simulation results; three sections, namely the AC, control scheme, and DC side results, are considered.

5.2. Further Research

Further research should focus on:

- The real-time simulation of the system
- Hardware design and implementation of three-phase regenerative rectifiers.

REFERENCES

Abad, G., Lopez, J., Rodriguez, M.A. & Iwanski, G. 2011. *Doubly Fed Induction Machine*. New Jersey: John Wiley & Sons, Inc. https://onlinelibrary.wiley.com/doi/book/10.1002/9781118104965.

Acikgoz, H., Kececioglu, O.F., Gani, A., Yildiz, C. & Sekkeli, M. 2016. Improved Control Configuration of PWM Rectifiers based on Neuro - Fuzzy Controller. *SpringerPlus*, 5(1): 1–19. https://springerplus.springeropen.com/articles/10.1186/s40064-016-2781-5.

Aktaibi, A., Rahman, A.M. & Razali, A. 2016. A Critical Review of Modulation Techniques. *IEEE*: 5. https://www.semanticscholar.org/paper/A-Critical-Review-of-Modulation-Techniques-Aktaibi-Rahman/719ab9e1ca988bda64f0134a7e5ab28a4daa4724.

Badr, M.A., Atallah, A.M. & Bayoumi, M.A. 2015. Comparison between Aggregation Techniques for PMSG Wind Farm. In *Energy Procedia*. Elsevier B.V.: 1162–1173. https://www.sciencedirect.com/science/article/pii/S1876610215015271.

Behera, R.R. & Thakur, A.N. 2016. An Overview of Various Grid Synchronization Techniques for Single-Phase Grid Integration of Renewable Distributed Power Generation Systems. In *International Conference on Electrical, Electronics, and Optimization Techniques, ICEEOT 2016*. Chennai: IEEE: 2876–2880. https://ieeexplore.ieee.org/document/7755223.

Bensalah, A., Benhamida, M.A., Barakat, G. & Amara, Y. 2018. Large Wind Turbine Generators: State-of-the-Art Review. In *Proceedings - 2018 23rd International Conference on Electrical Machines, ICEM 2018*. 2205–2211. https://ieeexplore.ieee.org/document/8507165.

Bhatia, S.C. 2014. *Advanced renewable energy systems*. Woodhead Publishing India Pvt. Ltd. http://93.174.95.29/_ads/EECC97AFF3873945BE19078600007336.

Bhattacharya, M. 2014. Improvement of Power Quality Using PWM Rectifier. *International journal of scientific and Research Publications*, 4(7): 1–11. https://www.semanticscholar.org/paper/Improvement-of-Power-Quality-Using-PWM-Rectifiers-Bhattacharya/10f29330a7ef4155e8d2c1721f1823d33c8fde37.

Bhowmick, K. & Narvekar, M. 2018. Power Electronic Systems for the Grid Integration of Renewable Energy Sources: A Survey. *IEEE Journal of Emerging and Selected Topics in Power Electronics*, 673: 37–46. https://ieeexplore.ieee.org/document/1667898.

Bilgili, M., Ozbek, A., Sahin, B. & Kahraman, A. 2015. An Overview of Renewable Electric Power Capacity and Progress in New Technologies in The World. *Renewable and Sustainable Energy Reviews*, 49: 323–334. https://www.sciencedirect.com/science/article/abs/pii/S1364032115004189?via%3Dihub.

Binder, A. & Schneider, T. 2005. Permanent Magnet Synchronous Generators for Regenerative Energy Conversion - A Survey. *IEEE*. https://ieeexplore.ieee.org/document/1665858.

Blaabjerg, F. 2018. *Control of Power Electronic Converters And Systems*. 2th ed. Academic Press. http://93.174.95.29/_ads/EE2E49AC644A2014181C1571A649D623 6 January 2020.

Blaabjerg, F. & Ma, K. 2017. Wind Energy Systems, Reviews Application of Power Electronics in Wind Energy Systems. *IEEE Power and Energy Society*, 105(11): 2116–2131. http://linkinghub.elsevier.com/retrieve/pii/B9780123972705000133.

Bongiorno, M. & Svensson, J. 2007. Voltage Dip Mitigation Using Shunt-Connected Voltage Source Converter. *IEEE Transactions on Power Electronics*, 22(5): 1867–1874. https://ieeexplore.ieee.org/document/4300860.

Breeze, P. 2016a. Offshore Wind Turbine Technology. In *Wind Power Generation*. Elsevier Inc, Academic Press. https://www.sciencedirect.com/science/article/pii/B9780128040386000098?via%3Dihub.

Breeze, P. 2016b. *Solar Power Generation*. Joe Hayton. https://www.elsevier.com/books/solar-power-generation/breeze/978-0-12-804004-1.

Brito, R., Carvalho, A. & Gericota, M. 2015. A New Three-Phase Voltage Sourced Converter Laplace Model. In *Proceedings - 2015 9th International Conference on Compatibility and Power Electronics, CPE 2015*. IEEE: 160–166.

https://ieeexplore.ieee.org/document/7231066.
Caixeta, D.A., Guimarães, G.C. & Chaves, M.L.R. 2014. Modeling of a wind energy conversion system for dynamic analysis using alternative transients program. *Ciencia y Engenharia/ Science and Engineering Journal*, 23(1): 37–45. http://www.seer.ufu.br/index.php/cieng/article/view/26547.
Cao, W., Xie, Y. & T, Z. 2012. Wind Turbine Generator Technologies. In *Advances in Wind Power*. InTech. http://www.intechopen.com/books/advances-in-wind-power/wind-turbine-generator-technologies 8 January 2020.
Chakraborty, S. & Kramer, W.E. 2013. *Power Electronics for Renewable and Distributed*. S. Chakraborty & W. E. Kramer, eds. Springer. Chakraborty, Sudipta%0AKramer, William E.
Chen, Y. & Jin, X.M. 2006. Modeling and control of Three-Phase Voltage Source PWM Rectifier. In *Conference Proceedings - IPEMC 2006: CES/IEEE 5th International Power Electronics and Motion Control Conference*. 1459–1462. https://ieeexplore.ieee.org/document/4778239.
Chen, Z., Guerrero, J.M. & Blaabjerg, F. 2009. A review of the state of the art of power electronics for wind turbines. *IEEE Transactions on Power Electronics*, 24(8): 1859–1875. http://citeseerx.ist.psu.edu/viewdoc/download?doi=10.1.1.725.9787&rep=rep1&type=pdf .
Choe, S., Son, Y.K. & Sul, S.K. 2016. Control and Analysis of Engine Governor for Improved Stability of DC Microgrid Against Load Disturbance. *IEEE Journal of Emerging and Selected Topics in Power Electronics*, 4(4): 1247–1258. https://sci-hub.tw/10.1109/jestpe.2016.2597309.
Cubas, J., Pindando, S. & Manuel, C. 2014. Explicit Expressions for Solar Panel Equivalent Circuit Parameters Based on Analytical Formulation and the Lambert W-Function. *MDPI*, 7(10): 4098–4115.
Darbellay, A. 2014. Global and Regional Trends in Renewable Energy Contents. In *Regulating Credit Rating Agencies*. Elsevier: 205–206. http://93.174.95.29/_ads/98DF7F2A51FC02AEE67366C239B2070D.
Dincer, I. & Acar, C. 2015. A Review on Clean Energy Solutions for Better Sustainability. *International Journal of Energy Research*, 39: 585–606. https://onlinelibrary.wiley.com/doi/epdf/10.1002/er.3329.
DiPippo, R. 2015. *Geothermal Power Plants: Principles, Applications, Case Studies and Environmental Impact: Fourth Edition*. 3rd ed. Elsevier. http://93.174.95.29/_ads/261890738D7A9CA039E32473E0826E74.
Dıaz-Dorado, E., Cidra, J., Carrillo, C. & Montano, A.F.O. 2013. Review of power curve modelling for wind turbines. *Renewable and Sustainable Energy Reviews journal*, 21: 572–581. https://sci-hub.tw/https://www.sciencedirect.com/science/article/pii/S1364032113000439.
Egré, D. & Milewski, J.C. 2002. The Diversity of Hydropower Projects. *Energy Policy*, 30: 1225–1230. https://www.sciencedirect.com/science/article/abs/pii/S0301421502000836?via%3Dihub .
EIA- US Department of Energy. 2019. Ocean Thermal Energy Conversion - U.S. Energy Information Administration (EIA). https://www.eia.gov/energyexplained/hydropower/ocean-thermal-energy-conversion.php 22 December 2019.
Ellabban, O., Abu-Rub, H. & Blaabjerg, F. 2014. Renewable Energy Resources: Current Status, Future Prospects and Their Enabling Technology. *ELSEVIER Renewable and Sustainable Energy Reviews*, 39: 748–764. http://dx.doi.org/10.1016/j.rser.2014.07.113.
Esmaeilian, H.R., Fadaeinedjad, R. & Moschopoulos, G. 2014. Dynamic operation and Control of a Stand-Alone PEM Fuel Cell System. In *Conference Proceedings - IEEE Applied Power Electronics Conference and Exposition - APEC*. 3378–3384. https://sci-hub.se/10.1109/apec.2014.6803792.
Goh, C.S. 2019. Energy: Current Approach. In *Sustainable Construction Technologies Life-Cycle Assessment*. 409. https://www.sciencedirect.com/topics/engineering/wind-turbines 5 January 2020.

Gopalan, S. 2016. A Comparative Study of Control Techniques for Three Phase PWM Rectifier. In *Proceedings of the 10th International Conference on Intelligent Systems and Control, ISCO 2016*. IEEE: 1–8. https://ieeexplore.ieee.org/document/7727142.

Hannachi, M. & Benhamed, M. 2017. Modeling and Control of a Variable Speed Wind Turbine with a Permanent Magnet synchronous Generator. *IEEE 2017 International Conference on Green Energy Conversion Systems (GECS)*, (1). https://ieeexplore-ieee-org.libproxy.cput.ac.za/stamp/stamp.jsp?tp=&arnumber=8066251.

Hansen, A.D. & Margaris, I.D. 2014. Type IV Wind Turbine Model. *DTU Wind Energy*: 51.

Harshada, C.B. 2016. Review of Control Techniques of Three phase Boost Type PWM Rectifiers. *IJSR*, 78(96): 1021–1027. http://citeseerx.ist.psu.edu/viewdoc/download?doi=10.1.1.725.9787&rep=rep1&type=pdf.

Hassan, K.T. & Abdullah, M.K. 2015. Control Strategy for Three-Phase PWM Boost Rectifier Operating Under Different Supply Voltage Conditions. *Iraq J. Electrical and Electronic Engineering*, 11(1): 83–100. https://www.iasj.net/iasj?func=fulltext&aId=102717.

Hevia-Koch, P. & Jacobsen, H.K. 2019. Comparing Offshore and Onshore Wind Development Considering Acceptance Costs. *Energy Policy*, 125(February 2018): 9–19. https://doi.org/10.1016/j.enpol.2018.10.019.

Hong, S.J., Hyun, S.W., Kang, K.M., Lee, J.H. & Won, C.Y. 2018. Improvement of Transient State Response Through Feedforward Compensation Method of AC/DC Power Conversion system (PCS) based on Space Vector Pulse Width Modulation (SVPWM). *Energies*, 11(6): 121693718.

Jamma, M., Barara, M., Akherraz, M. & Enache, B.A. 2016. Voltage oriented control of Three-phase PWM Rectifier Using Space Vector Modulation & Input Output Feedback Linearization Theory. *Proceedings of the 8th International Conference on Electronics, Computers and Artificial Intelligence, ECAI 2016*: 1–8. https://ieeexplore.ieee.org/document/7861085.

Jonkman, J., van Dam, J., Forsyth, T. & Davis, D. 2003. Investigation of the IEC Safety Standard for Small Wind Turbine Design Through Modeling and Testing. *IEC*, (January): 340–350. https://www.nrel.gov/docs/fy03osti/33004.pdf.

Jung, J., Lee, W.J., Park, S., Kim, Y., Lee, C.J. & Han, C. 2017. Improved Control Strategy for Fixed-Speed Compressors in Parallel System. *Journal of Process Control*, 53: 57–69. https://www.sciencedirect.com/science/article/pii/S0959152417300331.

Jung, T.H., Gwon, G.H., Kim, C.H., Han, J., Oh, Y.S. & Noh, C.H. 2018. Voltage Regulation Method for Voltage Drop Compensation and Unbalance Reduction in Bipolar Low-Voltage DC Distribution System. *IEEE Transactions on Power Delivery*, 33(1): 141–149. https://sci-hub.tw/10.1109/tpwrd.2017.2694836.

Kakkar, S., Maity, T. & Ahuja, R.K. 2019. Performance Enhancement of Grid Connected PWM Rectifier Under Grid Disturbances. *International Journal of Engineering and Advanced Technology*, 8(3): 69–74.

Karimirad, M. 2014. *Offshore Energy Structures For Wind Power, Wave Energy and Hybrid Marine Platforms*. Springer. https://www.springer.com/gp/book/9783319121741.

Khaburi, D.A. & Nazempour, A. 2012. Design and Simulation of a PWM Rectifier Connected to a PM Generator of Micro Turbine Unit. *Scientia Iranica*, 19(3): 820–828. http://dx.doi.org/10.1016/j.scient.2011.09.017.

Knapczykf, M. & Pieńkowskif, K. 2006. Analysis of Pulse Width Modulation Techniques for AC/DC Line-Side Converters. *Prace Naukowe Instytutu Maszyn*, (59).

Kondylis, G.P., Vokas, G.A., Anastasiadis, A.G. & Konstantinopoulos, S.A. 2017. Application of Voltage Oriented Control Technique in a Fully Renewable, Wind Powered, Autonomous System with Storage Capabilities. *AIP Conference Proceedings*, 1814. https://aip.scitation.org/doi/10.1063/1.4976285.

Kuang, C., Huang, H., Pan, Y. & Gu, J. 2012. A Literature Review of Tidal Power Generation with Coastal Reservoir. *Advanced Materials Research*, 512: 900–904. https://www.researchgate.net/publication/272598251_A_Literature_Review_of_Tidal_Power_Generation_with_Coastal_Reservoir.

Kumar, M.M. & Sundareswaran, R. 2015. PMSG Based Wind Energy Conversion with Space Vector Modulation. *International Journal of Energy and Power Engineering*, 4(3): 146–

152. https://pdfs.semanticscholar.org/f8af/4be4427daac9c7ee425b1c1ed3fc7194acd3.pdf.
Kumar, Y., Ringenberg, J., Depuru, S.S., Devabhaktuni, V.K., Lee, J.W., Nikolaidis, E., Andersen, B. & Afjeh, A. 2016. Wind Energy: Trends and Enabling Technologies. *Renewable and Sustainable Energy Reviews*, 53: 209–224. https://www.sciencedirect.com/science/article/abs/pii/S1364032115009016.
Kwasinski, A., Krein, P.T. & Chapman, P.L. 2003. Time Domain Comparison of Pulse-Width Modulation Schemes. *IEEE Power Electronics Letters*, 1(3): 64–68. https://ieeexplore.ieee.org/document/1257348 8 January 2020.
Letcher, T.M. 2017. *Wind Energy Engineering A Handbook for Onshore and Offshore Wind Turbines*. T. M. Letcher, ed. London: Elsevier. http://booksdescr.org/ads.php?md5=886d3a31b225ce729f3845011473ab5e.
Liang, J. & Feng, C.M. 2015. Advanced AC and DC Technologies to Connect Offshore Wind Farms into Electricity Transmission And Distribution Networks. In J.-L. Bessède, ed. *Eco-friendly Innovation in Electricity Transmission and Distribution Networks*. Elsevier Inc.: 263–290. https://www.sciencedirect.com/science/article/pii/B9781782420101000136 8 January 2020.
Liu, Z. 2015. *Global Energy Interconnection*. Jonathan Simpson. http://93.174.95.29/_ads/6BDA5560F27BECFF69E84738FDDD7A51.
Luque, A. & Hegedus, S. 2011. *Handbook of Photovoltaic Science and Engineering*. Wiley. http://93.174.95.29/_ads/8FAA012F2234351E170C6CA0AA01EB83.
Luta, D.N. 2014. *Modelling of Hybrid Solar Wind Integrated Generation Systems in An Electrical Distribution Network*. Cape Peninsula University of Cape Town. http://etd.cput.ac.za/bitstream/handle/20.500.11838/1177/212123254_luta_dn_mtech_elec_eng_2014.pdf?sequence=1&isAllowed=y.
Malinowski, M. 2001. *Sensorless Control Strategies for Three - Phase PWM Rectifiers*. Warsaw University of Technology. https://www.google.com/search?rlz=1C1CHZL_enZA764ZA764&sxsrf=ALeKk03fXK_PgOhG0e3TLo1dpPQV-jnIng%3A1600086714348&ei=umJfX5PmFILP1fAP3-WbgAE&q=Mariusz+Malinowsk-+Sensorless+control+strategies+for+three-phase+PWM+rectifiers&oq=Mariusz+Malinowsk-+Sensorless+c.
Malinowski, M., Kazmierkowski, M.P., Hansen, S., Blaabjerg, F. & Marques, G.D. 2001. Virtual-Flux-Based Direct Power Control of Three-Phase PWM Rectifiers. *IEEE Transactions on Industry Applications*, 37(4): 1019–1027. http://ieeexplore.ieee.org/document/936392/ 16 October 2020.
Malinowski, M., Kazmierkowski, M.P. & Trzynadlowski, A. 2003. Review and Comparative Study of Control Techniques for Three-Phase PWM Rectifiers. *Mathematics and Computers in Simulation*, 63(3–5): 349–361. https://www.sciencedirect.com/science/article/abs/pii/S0378475403000818.
Malinowski, M., Leon, J.I. & Abu-Rub, H. 2017. Solar Photovoltaic and Thermal Energy Systems: Current Technology and Future Trends. *Proceedings of the IEEE*, 105(11): 2132–2146. https://ieeexplore-ieee-org.libproxy.cput.ac.za/stamp/stamp.jsp?tp=&arnumber=7914744.
Manwell, J.F., Mcgowan, J.G. & Rogers, A.L. 2009. *Wind Energy Explained*. 2nd ed. John Wiley. http://booksdescr.org/ads.php?md5=503e993917a04b193e174f682669cf62.
Marian, K.P., Blaabjerg, F. & Krishnan, R. 2002. *Control in Power Electronics*. J. D. Irwin, ed. Elsevier.
Mittal, R., Sanddhu, K.S. & Jain, D.K. 2010. An Overview of Some Important Issues Related to Wind Energy Conversion System (WECS). *International Journal of Environmental Science and Development*, 1(4): 351–363. http://www.ijesd.org/papers/69-D467.pdf 8 January 2020.
Mohanty, P., Muneer, T. & Gago, E.J. 2016. *Solar Photovoltaic System Applications*. http://link.springer.com/10.1007/978-3-319-14663-8.
Muljadi, E., Singh, M. & Gevorgian, V. 2013. Wind Turbines Providing Spinning Reserves to the Grid Preprint. *IEEE Power and Energy Society*, (November 2012).
Navpreet, T., Tarun, M., Amit, B., Kotturu, J., Bhupinder, S., Anant, B. & Gurangel, S. 2012. Voltage Source Converters as The Building Block Of HVDC and FACTS Technology in

Power Transmission System: A Simulation based Approach. *Pelagia Research Library Advances in Applied Science Research*, 3(5): 3263–3278. www.pelagiaresearchlibrary.com.

Nayar, C. V., Islam, S.M., Dehbonei, H., Tan, K. & Sharma, H. 2011. Power Electronics for Renewable Energy Sources. In M. H. Rashid, ed. *Alternative Energy in Power Electronics*. Elsevier Inc.: 1–79. https://www.sciencedirect.com/science/article/pii/B9780124167148000019 8 January 2020.

Neill, S.P. & Hashemi, M.R. 2018. Offshore Wind. In S. P. Neill & M. R. Hashemi, eds. *Fundamentals of Ocean Renewable Energy*. Elsevier: 83–106. https://www.sciencedirect.com/science/article/pii/B9780128104484000045 8 January 2020.

Owusu, P.A. & Asumadu-Sarkodie, S. 2016. A Review of Renewable Energy Sources, Sustainability Issues and Climate Change Mitigation. *Cogent Engineering*, 3(1): 1–14. http://dx.doi.org/10.1080/23311916.2016.1167990.

Pao, L.Y. & Johnson, K.E. 2011. Control of Wind Turbines. *IEEE*: 44–62. https://ieeexplore-ieee-org.libproxy.cput.ac.za/stamp/stamp.jsp?tp=&arnumber=5730721.

Pashaei, A. & Aydemir, M.T. 2014. Design and Implementation of a Pulse Width Modulated Rectifier for Industrial Applications. In *22nd Iranian Conference on Electrical Engineering, ICEE 2014*. 574–579. https://www.researchgate.net/publication/263550953_Design_and_implementation_of_a_pulse_width_modulated_rectifier_for_industrial_applications.

Phankong, N., Yuktanon, N. & Bhumkittipich, K. 2014. Aero-Structural Design and Optimization of a Small Wind Turbine Blade. *Energy Procedia*, 56: 574–583. http://dx.doi.org/10.1016/j.egypro.2014.07.195.

Poulopoulos, S.G. & Inglezakis, V.J. 2016. *Environment and Development: Basic Principles, Human Activities, and Environmental Implications*. http://linkinghub.elsevier.com/retrieve/pii/B9780444627339000083.

Pourrajabian, A., Amir, P., Afshar, N., Ahmadizadeh, M. & Wood, D. 2015. Aero-Structural Design and Optimization of a Small Wind Turbine Blade. *Renewable Energy*: 12. http://dx.doi.org/10.1016/j.renene.2015.09.002.

Qi, H., Wu, Y. & Bi, Y. 2014. The main parameters design based on three-phase voltage source PWM rectifier of voltage oriented control. In *Proceedings - 2014 International Conference on Information Science, Electronics and Electrical Engineering, ISEEE 2014*. 10–13. https://ieeexplore-ieee-org.libproxy.cput.ac.za/stamp/stamp.jsp?tp=&arnumber=6948057 23 September 2020.

Richter, A. 2019. The top 10 Geothermal Countries 2018 based on Installed Generation Capacity MWe. *ThinkGeoEnergy*. https://www.thinkgeoenergy.com/the-top-10-geothermal-countries-2018-based-on-installed-generation-capacity-mwe/ 19 December 2019.

Riveros, J.A., Prieto, J., Rivera, M. & Toledo, S. 2019. A Generalised Multifrequency PWM Strategy for Dual Three-Phase Voltage Source Converters. *MDPI energies*, 12: 1–13. https://sci-hub.tw/10.3390/en12071398.

Rodríguez, J.R., Dixon, J.W., Espinoza, J.R., Pontt, J. & Lezana, P. 2005. PWM Regenerative Rectifiers: State of the Art. *IEEE Transactions on Industrial Electronics*, 52(1): 5–22.

Saher, R. Bin. 2012. *Three Phase Boost Rectifier Design*. Universiti Tun Hussein Onn Malaysia. http://eprints.uthm.edu.my/2905/1/ROHAIZAN_BIN_SAHER_1.pdf.

Sanjuan, S.L. 2010. *Voltage Oriented Control of Three - Phase Boost PWM Converters Voltage Oriented Control of Three - Phase Boost PWM Converters*. Chalmers University of Technology. http://webfiles.portal.chalmers.se/et/MSc/SylvainLECHATSANJUANMSc.pdf.

Sarasu, J.I., Fraile-ardanuy, J., Perez, J.I., Wilhelmi, J.R. & Jose, A. 2007. Control of a Run of River Small Hydro Power Plant. *IEEE*: 672–677. https://ieeexplore-ieee-org.libproxy.cput.ac.za/stamp/stamp.jsp?tp=&arnumber=4380132.

Sau-Bassols, J., Prieto-Araujo, E., Galceran-Arellano, S. & Gomis-Bellmunt, O. 2016. Operation and control of a Current Source Converter Series Tapping of an LCC-HVDC Link for Integration of Offshore Wind Power Plants. *Elsevier Electric Power Sysrems*

Research, 141: 510–521. http://dx.doi.org/10.1016/j.epsr.2016.07.019.
Scapini, R.Z., Bellinaso, L. V & Michels, L. 2018. Stability Analysis of AC-DC Full-Bridge Converters With Reduced DC-Link Capacitance. *IEEE Transactions on Power Electronics*, 33(1): 899–908. http://ieeexplore.ieee.org. 4 January 2020.
Schubel, P.J. & Crossley, R.J. 2012. Wind Turbine Blade Design. *MDPI energies*: 3425–3449.
Shahariar, G.M.H. & Hasan, M.R. 2014. Design & Construction of a Vertical Axis Wind Turbine. *IEEE 2014 9th International Forum on Strategic Technology, IFOST 20142014 9th*: 326–329.
Simani, S. 2015. Overview of Modelling and Advanced Control Strategies for Wind Turbine Systems. *MDPI energies*: 13395–13418.
Stephen, A.A. 2017. *Assessment of Renewable Energy*. University of Cape Town. https://open.uct.ac.za/bitstream/item/14604/thesis_ebe_2015_akinyemi_ayodeji_stephen.pdf?sequence=1.
Subhashini, S. & Sankari, C. 2014. Design and Control of Boost Converter for Renewable Energy Sources. *IOSR Journal of Electrical and Electronics Engineering*, 9(2): 07–18. http://www.iosrjournals.org/iosr-jeee/Papers/Vol9-issue2/Version-4/B09240718.pdf.
Sumathi, S., Ashok Kumar, L. & Surekha, P. 2015. *Solar PV and Wind Energy Conversion Systems: An Introduction to Theory, Modeling with MATLAB/SIMULINK, and the Role of Soft Computing Techniques*. Springer International Publishing,. http://link.springer.com/10.1007/978-3-319-14941-7.
Tagare, D.M. 2011. *Electric Power Generation*. John Wiley & Sons, Inc. http://93.174.95.29/_ads/96F50195BB782F6AA1D22C4D828850CC.
Tawfiq, K.B., Mansour, A.S., Ramadan, H.S., Becherif, M., Pina, A., Ferrão, P., Fournier, J., Lacarrière, B. & Corre, O. Le. 2019. Wind Energy Conversion System Topologies and Converters: Comparative Review. *Elsevier Energy Procedia*, 162: 38–47. https://doi.org/10.1016/j.egypro.2019.04.005.
Teodorescu, R., Liserre, M. & Rodriguez, P. 2011. *Converters for Photovoltaic and Wind Power Systems*. John Wiley & Sons, Inc.
Thorpe, D. 2015. New Study Identifies How Cities Can Cut Energy Use by 25% by 2050. *The Sustainable Cities Collective.*: 1. https://www.smartcitiesdive.com/ex/sustainablecitiescollective/new-study-identifies-how-cities-can-cut-energy-use 25-2050/1036406/ 4 March 2019.
Timbus, A., Teodorescu, R., Blaabjerg, F. & Liserre, M. 2005. Synchronization Methods for Three Phase Distributed Power Generation Systems. An Overview and Evaluation. In *PESC Record - IEEE Annual Power Electronics Specialists Conference*. IEEE: 2474–2481. https://www.researchgate.net/publication/224626835_Synchronization_Methods_for_Three_Phase_Distributed_Power_Generation_Systems_An_Overview_and_Evaluation.
Tong, W. 2010. Fundamentals of Wind Energy. In *Wind Power Generation and Wind Turbine Design*. Virginia,USA: WIT Transactions on State of the Art in Science and Engineering. https://www.witpress.com/Secure/elibrary/papers/9781845642051/9781845642051001FU1.pdf.
Towler, B.F. 2014. *The Future of Energy*. Elsevier Inc, Academic Press. http://93.174.95.29/_ads/C2C8B2233B8F85909C7AE5C2BE0DCAF7.
Trinh, Q.N., Wang, P. & Choo, F.H. 2017. An Improved Control Strategy of Three-Phase PWM Rectifiers under Input Voltage Distortions and DC-Offset Measurement Errors. *IEEE Journal of Emerging and Selected Topics in Power Electronics*, 5(3): 1164–1176. https://www.mdpi.com/1996-1073/11/6/1468/htm.
Trinh, Q.N., Wang, P., Member, S. & Choo, F.H. 2017. An Improved Control Strategy of Three-Phase PWM Rectifiers Under Input Voltage Distortions and DC-Offset Measurement Errors. *IEEE Journal of Emerging and Selected Topics in Power Electronics*, 5(3): 1164–1176.
Vázquez, N. & Vázquez, J. 2018. Power Generation and Distribution. In 4th, ed. *Power Electronics Handbook*. Elsevier. https://www.sciencedirect.com/topics/engineering/grid-connected-photovoltaic-systems 4 January 2020.
Walling, R.A., Gursoy, E. & English, B 2012. Current Contributions from Type 3 and Type 4 Wind Turbine Generators During Faults. *IEEE*, 5(12): 1–6. https://sci-

hub.tw/https://ieeexplore.ieee.org/stamp/stamp.jsp?tp=&arnumber=6281623.
Wang, C.N., Lin, W.C. & Le, X.K. 2014. Modelling of a PMSG Wind Turbine with Autonomous Control. *Mathematical Problems in Engineering*, 2014. https://www.researchgate.net/publication/274919318_Modelling_of_a_PMSG_Wind_Turbine_with_Autonomous_Control.
Wang, X., Yu, J., Bai, B. & Chen, D. 2013. Parameter Analysis and Calculation of Inductor for PWM Rectifier. In *Proceedings - 2013 International Conference on Mechatronic Sciences, Electric Engineering and Computer, MEC 2013*. Institute of Electrical and Electronics Engineers Inc.: 3822–3826. http://ieeexplore.ieee.org/lpdocs/epic03/wrapper.htm?arnumber=6885655 17 September 2020.
Wang, Y., Meng, J., Zhang, X. & Xu, L. 2015. Control of PMSG-Based Wind Turbines for System Inertial Response and Power Oscillation Damping. *IEEE Transactions on Sustainable Energy*, 6(2): 565–574. https://ieeexplore.ieee.org/document/7042817.
Wei, Q., Wu, B., Xu, D. & Zargari, N.R. 2017. A Medium-Frequency Transformer-Based Wind Energy Conversion System Used for Current-Source Converter-Based Offshore Wind Farm. *IEEE Transactions on Power Electronics*, 32(1): 248–259.
Whitby, B., Member, S. & Ugalde-loo, C.E. 2014. Performance of Pitch and Stall Regulated Tidal Stream Turbines. *IEEE Transactions on Sustainable Energy*, 5(1): 64–72.
Yusoff, N.A., Razali, A.M., Karim, K.A., Sutikno, T. & Jidin, A. 2017. A Concept of Virtual-Flux Direct Power Control of Three-Phase AC-DC Converter. *International Journal of Power Electronics and Drive Systems*, 8(4): 1776–1784. https://www.researchgate.net/publication/322347356_A_Concept_of_Virtual-Flux_Direct_Power_Control_of_Three-Phase_AC-DC_Converter.
Zhang, Y., Li, Y.W., Zargari, N.R. & Zhongyuan, C. 2014. Improved Selective Harmonics Elimination (SHE) Scheme with Online Harmonic Compensation for High- Power PWM Converters. In *IEEE*. 5510–5517. https://ieeexplore.ieee.org/document/6873315.
Zhang, Y. & Qu, C. 2015. Direct Power Control of a Pulse Width Modulation. *IEEE Transactions on Power Electronics*, 30(10): 5892–5901. https://ieeexplore-ieee-org.libproxy.cput.ac.za/stamp/stamp.jsp?tp=&arnumber=6960913.
Zhao, J. & Jiang, Q. 2017. Research on a New Control Strategy for Three-Phase Current-Source PWM rectifier. In *2017 8th International Conference on Intelligent Control and Information Processing, ICICIP 2017*. Hangzohou, China: 157–161. https://ieeexplore.ieee.org/document/8113934.
Zhao, Y. & Ding, C. 2018. Wind Power Generator Output Model Based on the Statistical Wind Speed Distribution Derived From the Historical Data. In *2018 2nd IEEE Conference on Energy Internet and Energy System Integration (EI2)*. IEEE: 1–5. https://ieeexplore-ieee-org.libproxy.cput.ac.za/stamp/stamp.jsp?tp=&arnumber=8582590.